



Deposited via The University of Leeds.

White Rose Research Online URL for this paper:

<https://eprints.whiterose.ac.uk/id/eprint/178505/>

Version: Accepted Version

Article:

Chapman, RJ, Moles, NR, Bluemel, B et al. (2022) Detrital Gold as an Indicator Mineral. Geological Society Special Publication, 516. pp. 313-336. ISSN: 0305-8719

<https://doi.org/10.1144/sp516-2021-47>

© 2021 The Author(s). Published by The Geological Society of London. All rights reserved. This is an author produced version of an article, published in Geological Society Special Publications. Uploaded in accordance with the publisher's self-archiving policy.

Reuse

Items deposited in White Rose Research Online are protected by copyright, with all rights reserved unless indicated otherwise. They may be downloaded and/or printed for private study, or other acts as permitted by national copyright laws. The publisher or other rights holders may allow further reproduction and re-use of the full text version. This is indicated by the licence information on the White Rose Research Online record for the item.

Takedown

If you consider content in White Rose Research Online to be in breach of UK law, please notify us by emailing eprints@whiterose.ac.uk including the URL of the record and the reason for the withdrawal request.

Accepted Manuscript

Geological Society, London, Special Publications

Detrital Gold as an Indicator Mineral

Robert J. Chapman, Norman R. Moles, Britt Bluemel & Richard D. Walshaw

DOI: <https://doi.org/10.1144/SP516-2021-47>

To access the most recent version of this article, please click the DOI URL in the line above. When citing this article please include the above DOI.

Received 5 March 2021

Revised 28 July 2021

Accepted 7 September 2021

© 2021 The Author(s). Published by The Geological Society of London. All rights reserved. For permissions: <http://www.geolsoc.org.uk/permissions>. Publishing disclaimer: www.geolsoc.org.uk/pub_ethics

Supplementary material at <https://doi.org/10.6084/m9.figshare.c.5625450>

Manuscript version: Accepted Manuscript

This is a PDF of an unedited manuscript that has been accepted for publication. The manuscript will undergo copyediting, typesetting and correction before it is published in its final form. Please note that during the production process errors may be discovered which could affect the content, and all legal disclaimers that apply to the book series pertain.

Although reasonable efforts have been made to obtain all necessary permissions from third parties to include their copyrighted content within this article, their full citation and copyright line may not be present in this Accepted Manuscript version. Before using any content from this article, please refer to the Version of Record once published for full citation and copyright details, as permissions may be required.

Detrital Gold as an Indicator Mineral

Robert J. Chapman¹, Norman R. Moles², Britt Bluemel³, Richard D. Walshaw¹

1. Ores and Mineralization Group, School of Earth and Environment, University of Leeds, Leeds LS29JT

2. School of Environment and Technology, University of Brighton, Lewes Road, Brighton BN2 4GJ, UK

3. Goldspot, 69 Yonge St, Suite 1010, Toronto, ON M5E 1K3 *Corresponding Author (e mail: r.j.chapman@leeds.ac.uk)

Abstract

Detrital gold fulfils the criteria of chemical inertia and physical durability required by indicator minerals but it has not found wide application in this role because it may be formed in different deposit types. This problem is soluble, because the generic compositional features of hydrothermal gold differ according to mineralization environment. The wide distribution of gold as a minor component of mineralization where other commodities are the principle exploration target extends the potential of an indicator methodology based on detrital gold to beyond the search for gold itself. Here we highlight how distinctive gold compositional signatures derived from alloy composition and deposit- specific suites of mineral inclusions could contribute to exploration for Cu-Au porphyries, redox- controlled uranium mineralization and ultramafic-hosted PGE mineralization.

Future refinement this approach will focus on establishing the spatial distribution of elements at trace levels within gold particle sections using ToF-LA-ICP-MS and application of Exploratory Data Analysis to the resulting data sets. This approach is in its infancy, but aims to develop a classification algorithm useful to researchers irrespective of their previous experience. A pilot study has that random forests provide the best approach to establishing gold particle origins.

Introduction

The increasing challenges in discovering new mineral resources have encouraged the development of indicator mineral methodologies designed to detect the presence of orebodies whose outcrop is obscured by surface cover. In this contribution, we examine the potential for compositional and mineralogical features of particulate gold to underpin indicator mineral methodologies both for the exploration of gold itself and for some other metalliferous mineralization where gold is an accessory.

The history of gold compositional studies may be roughly subdivided into four categories that seek to:

- i. establish placer-lode relationships in specific geographic areas (e.g. Knight et al. 1999a; Potter and Styles 2003; Moles and Chapman 2019; Lalomov et al. 2016)
- ii. characterise gold formed in specific deposit types according to generic compositional criteria (e.g. Morrison et al 1991; Townley et al. 2003; Chapman et al. 2017; 2018)
- iii. investigate modification to gold particles in the surficial environment (e.g. Groen et al 1990; Stewart et al. 2017; Reith et al. 2018)
- iv. interpret gold mineralogy in terms of specific constraints on conditions of mineralization to illuminate ore deposit studies (e.g. Chapman and Mortensen 2006; Chapman et al. 2009).

Knowledge gained from studies in the first two categories underpins this contribution. In addition, we address the implications of studies within the third category.

The importance of indicator mineral studies in exploration

Both geochemical and geophysical methods are routinely employed in the search for mineral deposits in areas where outcrop exposures are scarce. Geochemical methods traditionally include the determination of indicator mineral abundance in rock, soil, glacial or stream sediment (e.g., Averill 2001; McClenaghan and Paulen 2018 and references therein). The trace element geochemistry of various detrital minerals has been utilised to vector towards specific styles of mineralization. Copper porphyry deposits have been the focus of much of this research (e.g., Cooke et al. 2017, Plouffe and Ferbey 2017, Wilkinson et al. 2020) with a number of specific minerals investigated for their capacity to act as indicators, e.g. magnetite (Celis et al. 2014, Pisiak et al. 2017), apatite (Bouzari et al. 2010, 2016; Mao et al. 2016), and tourmaline (Chapman et al. 2015). Similar research on indicator minerals has been applied to other ore systems including kimberlite (McClenaghan and Kjarsgaard, 2007), magmatic Ni-Cu-PGE (e.g. Averill 2011, Barnett and Averill, 2010), volcanogenic massive sulphides (McClenaghan et al. 2015), and gold (e.g. Averill, 2017; Manéglija et al. 2018).

The criteria that makes an indicator mineral useful include a clear link to the source mineralization, or component thereof, chemical stability such that the particle endures in the surficial environment, and physical resilience to reduce obliteration by comminution. Detrital gold fulfils these requirements, and its presence in surficial sediments is widely regarded as

an indicator of proximity to local/regional hypogene mineralization (McClenaghan and Cabri, 2011).

Perceived issues with using gold as an indicator mineral

Correlation of physical characteristics of gold particles with abundance in glacial dispersal trains have been interpreted to provide vectors to source (e.g., Averill 2001; Girard et al., 2021) but for several reasons the compositional characteristics of gold in fluvial placers have not been routinely exploited in exploration programs. These can be summarised as:

- (1) The strong spatial relationship between particle abundance and source which underpin studies of dispersal trains in glacial sediments break down quickly in fluvial settings where the segregation of gold particles into different fluvial facies may be pronounced, the degree of transport may be far greater and the capacity for ingress of gold from other sources increased.
- (2) In many orogenic belts different deposit types occur within the catchment of a single drainage and hence the presence of gold particles in sediment does not facilitate targeting of a specific deposit type.
- (3) The physical and compositional properties of gold may vary substantially within a single deposit, which can further obfuscate the relationship between detrital gold particles and their source.
- (4) The extreme chemical and physical durability of gold facilitates recycling to successive surficial environments. In areas where the current fluvial system is superimposed onto sediments laid down in a different palaeo-drainage regime, the transport history of gold particles may be unclear and their value as a vector to source diminished (Plouffe et al. 2016, 2017).
- (5) Some authors strongly advocate gold growth by biogeochemical processes (e.g., Reith et al. 2018). These studies resonate with a widely held perception that in general the particle size of gold in placer environments is larger than that of the hypogene source (e.g., Boyle 1979), and that remobilization and reprecipitation is the most likely explanation. If this hypothesis is correct there would be a clear disconnect between the mineralogy of hypogene gold and the erosional products which would fatally undermine the use of particulate gold as an indicator.
- (6) The changing hydrodynamic behaviour of gold with decreasing particle size precludes either concentration of particles of below 50 μm from a sand/gravel matrix in specific fluvial settings and efficient separation by gravity separation methods. Many economically important gold deposits contain gold particles smaller than this and consequently do not generate a local placer expression to act as a vector to source. To summarise, the apparent lack of ability to link detrital gold to a specific source coupled with uncertainty of the genetic relationship has negatively influenced opinion on the suitability of gold as an indicator mineral.

Our increased understanding of the compositional characteristics of particulate gold (i.e. alloy composition and inclusions of other minerals indicative of source mineralogy) and their relationship to specific styles of mineralization provides a platform to overcome the potential disadvantages outlined in 1-6 above. Regarding point 5, we acknowledge that specific chemical environments may facilitate gold mobility as a thiosulphate complex, such as in supergene environments containing circum-neutral groundwaters in New Zealand (e.g., Craw

and Kerr 2017) and in arid terranes due to seasonal variation in the water table (Dunn et al. 2019). Nevertheless, we routinely observe the same compositional profiles, inclusion suites and heterogeneous microfabrics in gold particles liberated directly from ore and in associated placer gold. The near ubiquitous occurrence of these features in gold from placer environments coupled with the absence of any features that indicate gold growth in situ underpin our assertion that in the overwhelming majority of cases placer gold represents the erosional product of a hypogene source. This subject is discussed in detail in a companion paper within this volume (Chapman et al. 2021a).

The present contribution describes previous considerations of the potential application of gold as an indicator mineral, our current understanding of the characteristics of natural gold that could refine future approaches, the analytical techniques that could be applied, and novel approaches to data interrogation.

Terminology

In the last 50 years, various researchers have undertaken gold compositional studies and this has resulted in the use of different nomenclature. Chapman et al. (2021b) provide suggestions for a standardized terminology, and the present contribution has adopted those recommendations. Most importantly, the term ‘gold alloy’ is used to describe the composition of natural gold rather than ‘fineness’ ($\text{Au} \times 1000/(\text{Au}+\text{Ag})$) or ‘electrum’ as neither take into account the presence of other minor alloy components which may be informative. The word ‘gold’ is used to describe the mineral whereas ‘Au’ refers to the element, e.g. ‘wt. % Au in an alloy’. The term ‘gold grain’ is used here in its metallurgical sense: i.e. a definable crystal domain (Chapman et al. 2021b) and a ‘gold particle’ describes a single physical entity that typically comprises multiple gold grains (in contrast to previous publications which use the term ‘gold grain’ as meaning a particle). The term ‘sample population’ is used to describe a batch of gold particles collected from a specific locality. The ‘signature’ of a sample population is a synthesis of an array of the distinctive compositional features.

History of gold compositional studies in placer-lode investigations

The variation in silver content of gold from different localities is well known (e.g. Boyle 1979). In some placer mining districts, fineness values govern the remuneration for miners, and historic records are available. Comprehensive historical data describing bulk gold compositions can provide a useful insight into variations in regional gold mineralization, and have been used to illuminate the relationships between placer deposits and potential sources (e.g. Fisher 1945) and to characterize genetic relationships between gold sources in orogenic gold fields (Chapman and Mortensen 2016). Consideration of bulk values alone can neither indicate the range of compositions nor the presence of multiple sub populations, whereas both are brought into sharp focus through establishing a signature through the characterization of multiple individual particles from the same locality. This approach has been facilitated by rapid data acquisition afforded by the application of electron microprobe analysis (EPMA). The use of EPMA is particularly appropriate where gold particle sections are heterogeneous, because of the operator has control on the specific site of analysis. Chapman et al. (2021b) differentiated between gold formed in the primary environment of metal precipitation and that formed at a later date (see discussion below). Generally, analysis of the primary alloy

may be achieved by consideration of microfabrics revealed in polished section, and choice of appropriate analysis site. Early EPMA studies of polished gold sections also revealed the presence of other minor alloying elements, such as Cu (Antweiler and Campbell 1977), Pd, (Leake et al. 1991) and Hg (Knight et al. 1999a), whose presence at detectable levels provides valuable additional discriminants.

Preparation of polished sections of gold particles also reveals internal heterogeneity which cannot otherwise be inferred. Several workers reported the presence of mineral inclusions (e.g., Knight et al. 1999a; Youngson and Craw 1995; Loen 1994; 1995) but the first systematic approach to recording the suite of inclusions and utilising the data as a means of characterization was developed by Leake et al. (1992). The dual approach of combining inclusion assemblages with alloy composition was adopted by Chapman et al. (2000) to characterize variation in gold from orogenic settings throughout the UK and Irish Caledonides. A study of placer-lode relationships in the Klondike, Yukon Canada based on alloy compositions alone (Knight et al. 1999a) was refined through systematic studies of inclusion suites (Chapman et al. 2010a,b). Additionally, inclusion suites have proved the best diagnostic criteria to develop generic compositional templates for gold formed in both calc-alkaline and alkalic porphyry systems (Chapman et al. 2017, 2018). Where populations of placer gold are a composite of gold from distinct sources, considerations of alloy signatures and potentially diagnostic inclusions can permit informed speculation on the source deposit types. This approach has recently found application in placer districts where knowledge of the regional metallogeny may be incomplete, e.g. Cameroon (Omang et al. 2015; Dongmo et al. 2018), Pakistan (Alam et al. 2018) and/or specific placer-lode relationships unclear, e.g. Russia (Lalomov et al. 2017; Nevolko et al. 2019).

The ability to determine elemental concentrations at trace and ultra-trace levels using laser ablation inductively-coupled plasma mass spectrometry (LA-ICP-MS) has provided an enticing prospect for the study of natural gold because of the potential to utilize a wider range of discriminants for characterization. To date the approach has been limited largely to the use of quadrupole-MS systems. Initial studies of gold bullion using this technique (Watling et al. 1994) showed that trace element fingerprints could match smelted gold to source throughout Western Australia. Characterization of spatial variation of heterogeneity in gold particles using the quadrupole system is challenging because the mass spectrometer analyses individual elements sequentially, such that small-scale elemental covariance may escape detection. Studies on a large number of gold particles by Banks et al. (2018) suggest that the sequential ablation of natural gold particles generated elemental responses which could be explained by: i. alloy components distributed heterogeneously, ii. small inclusions of other minerals and iii. localized concentrations of elements within the alloy (defined as 'clusters' by Chapman et al. (2021b)). The development of time of flight (ToF) systems for element analysis permitted mapping trace element distribution on polished particle surfaces and confirmed the common but sporadic presence of clusters. These observations substantiate the larger data sets from LA-ICP-MS using the quadrupole system, where regular low signal responses of various elements do not necessarily suggest ablation or part ablation of particulate mineral inclusions (Banks et al. 2018).

Characteristics of natural gold that permit compositional characterization

Gold is most commonly an alloy of Au and Ag (Ag typically 5-30 wt%) which may or may not contain Hg, Cu and Pd to concentrations detectable by EPMA (typically 0.3 wt%, 0.02 wt% and 0.02 wt% respectively (Chapman et al. 2021b). A detailed account of the internal heterogeneity in natural gold both with respect to alloy composition and inclusions of other minerals is also provided by Chapman et al. (2021b), and a brief summary is included here. Textures characteristic of alloy heterogeneity are observed in gold particles from many different localities and some examples are illustrated in Figure 1.

Chapman et al. (2021b) classified these features according to the timing of their formation. Initial alloy composition (site 1 Fig. 1A) and inclusions of 'ore' minerals such as sulphides, sulpharsenides, sulphosalts, tellurides and selenides (example in Fig 1B) are primary features controlled by the initial environment of precipitation. The Au/Ag ratio is a function of both solution chemistry (pH , fS_2 , fCl_2 , Au/Ag_{aq}) and temperature (Gammons and Williams-Jones 1995). Controls on the concentrations of other minor elements have not been established in the same way, but are also likely influenced by equilibrium considerations governed by the various aqueous metal complexes. Chudnenko and Palyanova (2016) showed that the maximum Cu content of Au-Ag alloy is controlled by the Ag content and several studies (e.g., Chapman et al. 2017; Dongmo et al. 2018) reported an inverse relationship between Ag and Cu in Au alloy in particles from the same locality. Presently it remains unclear whether the commonly observed range (typically < 0.5 wt%) of Cu contents of gold alloy is primarily controlled by fluid composition or by Ag content of the alloy, or whether the controlling influence is the same in all cases.

Primary gold alloy may be modified within the hypogene environment by interaction with later fluids with which it is not in equilibrium. Compositional changes may manifest as patches or tracks of Ag-rich alloy (e.g. site 2, Fig 1A) and occasionally modified alloy contains a distinctive inclusion suite, such as wittichinite (Cu_3BiS_3) and hessite ($AgTe_2$) inclusions occurring within Ag-rich gold alloy from Borland Glen in the Ochil Hills, Scotland (Fig. 1C and Chapman and Mortensen, 2006). Alloy modified in this way is almost always richer in Ag than the original metal, most likely as a consequence of lower $Au/Ag_{(alloy)}$ values in the fluid and/or a lower temperature (Gammons and Williams-Jones 1995). Distinctive patterns of Au/Ag zonation observed in many gold particles (e.g. Fig 1D) can be attributed to alloy modification by grain boundary migration in the presence of a fluid unrelated to the original hypogene event (Chapman et al. 2021b). Tracks of Au-rich alloy or pure Au (Fig 1E) are also spatially related to grain boundaries, but form in the surficial environment, often infilling cracks (Hough et al. 2009). Gold-rich rims on detrital gold particles (Fig 1F) are nearly ubiquitous and are a consequence of alloy alteration within the surficial environment. They consist of alloy containing <2% Ag, are of true thickness 2-10 μ m with a sharp interface with the grain core (e.g., Knight et al. 1999b). Their formation by Ag removal (Groen et al. 1990) places a limit on the extent of modification, unless further fluid access is facilitated by deformation associated with recycling into successive fluvial environments (Stewart et al. 2017).

Mineral inclusions are primary features (Figs 1B, C, H) and in most cases they correspond to components of ore mineralization (Chapman et al. 2000a). It is important to make a distinction between mineral inclusions formed in the hypogene setting and fragments of fluvial sediment that may appear to be ‘included’ within a gold particle when viewed in polished section. Hypogene inclusions form a continuous contact with their alloy host, whereas impacted particles are uncommon, but easily recognised by the presence of voids between the mineral and the gold host (Fig 1G:) and the alteration of the original gold to form a ‘rim’ shaped sympathetically to the ‘inclusion’. Furthermore, the impacted particles are always resistate minerals such as quartz or zircon, but never ore minerals because these are chemically unstable and do not persist in the surface environment. Inclusions within gold particles survive weathering environments and residence in the surficial environment and provide clear evidence of the mineral associations within the source. The mineralogy of the inclusion suite in a population of gold particles from a specific locality corresponds to that of the auriferous stage of the source mineralization (Chapman et al. 2000a).

Trace element mapping of polished particle surfaces using time of flight (ToF) LA-ICP-MS has shown that trace element heterogeneity in gold alloy takes three forms (Banks et al. 2018, Chapman et al. 2021a), and examples of each are presented in Figures 1 H-K. Figure 1H is a BSE image of a gold particle post-analysis by ToF-LA-ICP-MS with the matt surface being a consequence of the ablation pitting. The inclusions of pyrite are clearly visible, but the subsequent analysis by ToF-LA-ICP-MS revealed other inclusion species that variously contained Fe, Bi and in one case Te. Figure 1 I shows Pd concentrations of a similar magnitude in most of a particle section, indicating that Pd is an alloy component. Figure 1J shows localised, high intensity responses for Fe commensurate with the pyrite inclusions and lower intensity responses for inclusions A and B (Fig. 1H). Figure 1 K shows low intensity responses for Ir that are coincident only with similar signals for Pt (observed in a separate image, not shown here). The underlying reasons for element occurrence within either clusters or inclusions (i.e. discrete mineral particles of definable stoichiometry) are currently unclear, however, these relationships provide an avenue for future studies of gold depositional processes and potential additional discriminants to exploit in indicator mineral methodologies.

Approaches to characterising gold according to source style of mineralization

The applicability of detrital gold as an indicator mineral is dependent upon identification of generic compositional signatures that are diagnostic for gold formed in different geological settings. In this section we explore the various approaches that have been employed to characterise gold composition in relation to source style.

Morrison et al. (1991) examined the range of Ag contents in Au alloy from bullion generated from different mines in order to investigate relationships to deposit style. The data relate to bulk averages of alloy composition, but nevertheless some broad trends were identified, for example, the wide permissible range of Ag contents associated with epithermal mineralization. There is considerable overlap in Ag ranges exhibited by gold from orogenic, porphyry and epithermal settings, all of which can produce Ag contents in the range 0-20%.

The authors noted that the Cu content of gold was only commonly detectable by EPMA in gold from porphyry systems. Townley et al. (2003) characterised gold compositions according to populations of particles from various epithermal, Cu-Au porphyry and Au-rich porphyry deposits. The authors generated compositional fields using triangular diagrams with Au-(Ag x 10) and (Cu x 100) apexes (Fig. 2A). The study drew on data describing gold from many different localities to generate mutually exclusive compositional templates for gold from each deposit type. However, Moles et al. (2013) noted that the compositional field for gold from orogenic settings overlapped almost completely with that for 'epithermal gold' reported by Townley et al. (2003). Additionally, compositional data describing gold from the Celopech high sulfidation deposit, Bulgaria (Bonev et al. 2002) fall within the porphyry and epithermal fields (Fig. 2A). We conclude that it is not possible to define diagnostic compositional fields for all styles of mineralization based on major and minor elements detectable by EPMA.

The approach to gold particle characterization adopted by the British Geological Survey (BGS), combined data sets describing both alloy composition and mineral inclusions observed in polished section. Integration of these data sets on a particle-by-particle basis generated a 'microchemical signature' describing the whole population (Leake et al. 1992). These authors continued to use alloy compositions as a primary discriminant but showed that consideration of the stability fields of minerals present within the inclusion assemblage permitted constraint of the conditions of ore formation. The distinctive Au-Pd alloy signature and inclusion signatures dominated by Se- and Te-bearing minerals recorded in gold from Devon and Southern Scotland was key to the development of a deposit model involving remobilization of Au and Pd by oxidizing chloride brines in red bed sequences with subsequent redox-controlled metal precipitation (Leake et al. 1991). Application of the microchemical characterization technique has identified a range of signatures associated with gold from orogenic settings (e.g. Chapman et al. 2010a,b ; Chapman and Mortensen 2016) and distinctive signatures associated with gold from alkalic porphyry and calc-alkalic porphyry settings (Chapman et al. 2017 and 2018 respectively).

Graphical methods for depiction of compositional characteristics of gold particle populations

Comparison between compositional characteristics of mineral populations is a fundamental operation in indicator studies. Studies using EPMA for alloy analyses have adopted a range of approaches to depict variation of alloy compositions generated by analysis of a population of gold particles. Approaches to graphical representation of inclusion assemblages have become more sophisticated as successive studies have revealed the range of mineral species that may be present.

Depiction of alloy compositions of populations of gold particles using cumulative percentile plots has proved an effective means of comparing different data sets to elucidate the relationship between different sample populations. The use of the cumulative percentile function permits direct comparison of metal profiles in sample populations that contain different numbers of particles. In this case, gold particles from a vein system (BRX zone

Klaza, Yukon) contribute to the adjacent placer (particles containing < 25wt% Ag), but the placer sample also contains gold particles with a higher Ag component not represented in the vein samples. Alloy data describing Ag contents alone are rarely diagnostic for deposit type, but they are useful for establishing potential genetic relationships between sample populations collected from separate sites during regional studies (e.g., Leake et al. 1998, Knight et al. 1999a). Such data are also useful to evaluate compatibility of sample populations where there are advantages to combining inclusion data for samples from nearby sites (e.g., Chapman and Mortensen 2016). Cumulative Ag plots provide the best approach in this regard (Fig 2B).

Ternary diagrams (Fig 2A) and bivariate plots (Fig 2C) have also been deployed where minor alloying elements are detectable in sufficient particles to examine their covariance (e.g. Townley et al. 2003; Moles et al. 2013; Chapman et al. 2017). Triangular diagrams have several disadvantages, namely quantitative data are lost, analytical errors inherent in low values of minor elements are amplified when multipliers are used, and plotting both Ag and Au in effect plots the same variable twice if other components have low concentrations. Bivariate plots can show clear relationships between concentrations of minor elements without the need for normalization of data, e.g. the inverse relationship between Cu and Ag shown in Fig. 2C. They permit some multivariate analysis by choice of symbols to represent other characteristics of specific gold particles, such as provenance, other elements within the alloy, or specific inclusions, also shown in Figure 2C.

Where present, detectable concentrations of Cu, Hg and Pd either individually or in combination provide an independent source of evidence which is useful for ascribing source style (e.g. Townley et al. 2003; Moles et al. 2013; Chapman et al. 2009, 2017), and dedicated bivariate plots provide an efficient tool for graphical depiction.

Graphical illustration of inclusion assemblages has proved more challenging because of wide range of inclusions species that may be present, often coupled with small data sets resulting from low inclusion abundance. Irrespective of approach, data are obtained by a count of the gold particles that contain a specific mineral. No account is taken of the number of inclusions of that mineral observed in a particle section nor their size. Data that underpins graphical techniques involves considering the proportions of the inclusion suite defined by either mineralogical or chemical criteria: e.g., the proportion of the inclusion suite that contains pyrite, or the proportion of copper-bearing minerals.

Early studies commonly had limited inclusion suites at their disposal, and adopted classification by mineral class as a means to reducing the small and variable data sets to a state where they could be visually assimilated. Triangular diagrams provided the capability to consider three components simultaneously, (e.g. Chapman et al. 2000a) but complex inclusion assemblages required multiple triangles to depict 4 or more variables. Additional triangles were inevitably based on data sets too small to generate a meaningful semi-quantitative measure, and consequently some data was omitted from the graphical representation. Mitigation was partially achieved by designing bespoke diagrams, which combined mineral classes and individual minerals important in a specific study (e.g.,

Chapman and Mortensen 2016), but such figures preclude direct comparison of results between different studies. Spider diagrams showing the proportion of all mineral species present provided one solution, particularly when plot design accommodated common mineral associations to generate distinctive patterns in different parts of the plot (e.g., Chapman et al. 2017; Moles and Chapman 2019). The disadvantage of this approach is that comparison of more than three superimposed plots usually generates illegibility. A detailed evaluation of the various approaches to the depiction of inclusion assemblages is provided by Chapman et al (in press)

Consideration of the mineralogy of the inclusion suite often provides important information, particularly when individual minerals may provide a clear indication of deposit type (e.g. Chapman et al; 2017, 2018). In other cases, consideration of mineral stability fields may permit prediction of conditions of mineralization (e.g., Chapman and Mortensen 2006). In some cases, it is clear that the elemental profile of an inclusion suite can provide useful information, for example, elements such as Bi, Te and Sb are often present in different minerals. The cumulative effect of these elemental signatures can act as a valuable discriminant, but the impact of the data is diminished by considering each mineral species separately.

In order to facilitate direct comparison of inclusion suites in gold from different deposit types it is necessary to utilise a standard approach appropriate for all signatures and which facilitates rapid comparison. Accordingly, we have adopted the semi-quantitative approach to the representation of inclusion suites based on inclusion chemistry advocated by Chapman et al. (in press). The methodology is described briefly below but the reader is referred to Chapman et al. (in press) for a full account of the advantages of this approach with respect to other graphical methods.

The numbers of gold particles which contain each inclusion species are summed and a scoring system applied according to elemental composition. The total metal value of an inclusion is '1' as is the total non-metal value. Inclusions are scored according to simple rules of presence or absence, and the score is independent of stoichiometry. Whilst some mineralogical distinctions are lost (e.g., pyrite scores the same as pyrrhotite ($\text{Fe}=1, \text{S}=1$) and chalcopyrite the same as bornite ($\text{Cu}=\text{Fe}=0.5, \text{S}=1$)), the method has the advantage of ascribing a fractional score such as 0.1 for elements present as minor components of standard minerals: e.g., Sb-bearing galena, ($\text{Pb}=0.9, \text{Sb}=0.1, \text{S}=1$) or minor amounts of Te or Se substituting in sulphides. The use of radar diagrams (e.g. Fig 3B) depicting 11 metals and five non-metals and metalloids provides a single transferrable graphical approach to simultaneous consideration of 16 variables, and a log scale (axes of 1%, 10% and 100%) emphasises the influence of minor components which greatly aid characterization. Clearly, individual elemental signatures can be generated by different minerals, and it remains important to acknowledge the importance of specific mineral species. Nonetheless, the approach facilitates rapid comparison between any inclusion signatures using a single visual template, and the ensuing similarities between gold from different localities of the same deposit type underline the value of the approach within indicator studies (Figs. 3-5). Currently, our preferred approach to interpretation of inclusion data sets uses inclusion suite element distribution as

the primary discriminant but acknowledges the potential importance of specific minerals on a case-by-case basis.

Signatures of gold from different styles of mineralization

Source style of mineralization is normally deduced from compositional data describing sample populations through consideration of combined data sets from alloy and inclusion analysis. In other cases, specific minerals or heterogeneous alloy fabrics may be informative. Individual inclusion species are rarely absolutely diagnostic for a style of mineralization, but some, and particularly some combinations, are far more common in gold from specific environments (e.g., the inclusion signatures of gold from porphyry mineralization described by Chapman et al. 2017; 2018). We have been cautious in proposing generic criteria where only a few populations are available for comparison. Figures 3-5 provide summary data describing signatures of gold populations from styles of mineralization where sufficient data are available. Each figure provides alloy and inclusion data relating to populations of gold, together with examples of specific features that are commonly observed. An overview of compositional features according to source style is presented in Table 1.

Magmatic hydrothermal systems

This category includes porphyry systems (both calc-alkalic and alkalic), skarn, high and low sulphidation epithermal mineralization, intrusion-related Au, and gold associated with late stage hydrothermal processes in ultrabasic intrusions. A scoping study of signatures of gold hosted by Portuguese Variscan granites is provided by Leal et al. (2021). Currently, it is not possible to provide robust signatures for gold from either skarn or VMS mineralization because of the small number of data sets available. Nevertheless, the available evidence is consistent with the general principle of replication of ore mineralogy in the inclusion suite; for example, the Bi signature reported in the inclusion suite of gold from skarn mineralization at Veletanga, Equador (Potter and Styles, 2003).

Studies focussing on characterization of gold from porphyry systems have provided a platform for establishing genetic signatures (Chapman et al. 2017, 2018) and a parallel study of associated epithermal systems has provided some insights into compositional signatures associated with hydrothermal evolution in the porphyry-epithermal environment (e.g. Chapman et al. 2018). Further studies are warranted because the wide variation in P-T-X within epithermal systems has the potential to generate a variety of signatures, as shown by the widely different Ag ranges of gold from different low sulphidation epithermal gold occurrences depicted in Figure 3F.

Figure 3A presents examples of alloy and inclusion signatures for gold derived from porphyry-epithermal systems. Gold from calc-alkalic porphyry systems is represented by sample populations from the Casino and Nucleus/Revenue systems, Yukon, Canada, whereas alkalic porphyry mineralization is represented by the Copper Mountain area and Afton (British Columbia, Canada). Gold from the calc-alkalic systems most likely represents that formed in the porphyry stage, whereas placer gold from the Copper Mountain and Afton areas may contain contributions from both porphyry and epithermal environments. This

distinction provides an explanation for the differences in the slope of the Ag cumulative curves if increased Ag range correlates with the number of hydrothermal systems from which the gold derives. Consideration of the concentrations of minor metals can be more illuminating: for example, in the Canadian Cordillera, detectable Cu is common in gold particles from porphyry systems but very uncommon in gold from orogenic hydrothermal systems (Chapman et al. 2021b). Gold particles derived from alkalic porphyry systems commonly exhibit a Pd-Hg signature in which Hg is detectable by EPMA (i.e. >0.3 wt %) in all cases and Pd is recorded sporadically up to values of 11wt%. The inclusion suites for the various sample populations are also illustrated (Fig. 3B) and show differences according to porphyry type. A suite of minerals including galena, Bi-tellurides (Fig. 3C), altaite, tetradymite and cosalite generates the Pb-Bi-Te-S signature of the inclusion suite typical of gold formed in calc-alkalic porphyries in the Canadian Cordillera (Chapman et al. 2018). These features are less pronounced in gold from the alkalic porphyry systems but here Chapman et al. 2017 observed a generic Pd-Hg signature is evident through the presence of minerals such as temagamite (Pd_3HgTe_3) and isomertierite ($\text{Pd}_{11}\text{Sb}_2\text{As}_2$) (Fig. 3D). For all porphyry systems, molybdenite is a minor, but common component of the inclusion signature and Cu may be present as Cu sulphides in addition to chalcopyrite. Minerals with several element components (e.g. Fig. 3E) are far more common in gold formed in porphyry and epithermal magmatic hydrothermal systems than in gold from orogenic mineralization.

Examples of signatures of gold from low-intermediate sulphidation epithermal systems and associated features are illustrated in Figures 3F-I. The Ag cumulative plots in Figure 4F all show major sub-horizontal portions indicating stable conditions of precipitation according to the controls on alloy composition developed by Gammons and William-Jones (1995), but the Ag values vary considerably between gold from different localities. Morrison et al. (1991) noted a wide variation in the Ag contents of gold from epithermal systems, but this observation must not require a wide variation in Ag from individual occurrences. Inclusion mineralogy between localities is variable (Fig. 3G) and there may be strong contributions from either Te or Se (Figs. 3H, I). In general, where fractures in detrital gold particles permit access to oxidizing conditions, inclusions may decompose, e.g. goethite after pyrite is relatively common. The presence of some rarer mineral species such as Bi telluride may be inferred from specific secondary minerals as illustrated in Figure 4I. Base metals are represented, but the Cu values appear lower than those associated with porphyry mineralization. In general, the changes in inclusion suite associated with the porphyry – low sulphidation epithermal transition mirror the commonly observed mineralogical differences in that Cu decreases whilst Pb (\pm Zn) and Ag increase whereas the Bi and Te signatures appear diluted, but are retained (Chapman et al. 2018).

Only a limited amount of information is currently available on gold formed in high sulphidation epithermal systems. Unpublished data held by one of us (RC) shows that sample populations of detrital gold from the environs of the Celopech deposit in Bulgaria exhibit an inclusion signature containing chalcopyrite, covellite and bornite, which is compatible with descriptions of the ore mineralogy provided by Bonev et al. (2002). Some of the alluvial gold

described by Moles et al. (2013) contains significant Cu in the alloy as well as Cu sulphide inclusions, and may have also formed in a high sulphidation epithermal context.

Initial studies of the inclusion mineralogy of gold from intrusion-related gold systems have also shown sympathy with the deposit mineralogy. Inclusions of molybdenite (Fig 3J), arsenopyrite, and some Bi-bearing minerals have been observed in gold from Dublin Gulch, Yukon (Chapman et al. in press). The signature differed from that of gold from Yukon calc-alkalic porphyries because the presence of arsenopyrite inclusions generated a clear As component. This research is ongoing.

The compositions and textural features of Au-Ag alloy containing Cu to percent levels were investigated by Knight and Leitch (2001). Such high levels of Cu are most commonly associated with gold associated with ultramafic rocks, but may also be present as Au-Cu alloys in gold formed in low temperature oxidizing chloride hydrothermal systems (see section below). The high Cu content in the presence of Ag induces exsolution of tetraauricupride, AuCu, over long residence periods at low temperature (Knight and Leitch 2001). Figure 3K demonstrates the complexity of the exsolution texture and highlights the difficulties in generating a meaningful single analysis value. In this case the alloy texture is the defining feature, but it is supported by a distinctive inclusion mineralogy which is dominated by chalcocite (Fig. 3L) and bornite, together with various PGMs. The Au-PGM-copper sulphide association has also been recorded in gold from the lower Orange River, Namibia (RC unpublished data) both in the form of PGM inclusions within Au-Ag alloy, and gold inclusions within PGM particles (Fig. 3M).

Orogenic hydrothermal systems

Considerable attention has been devoted to defining deposit models for gold formed in orogenic belts of all ages (see Mortensen et al. this volume). The current consensus is that the term 'orogenic gold' provides an overarching category, primarily describing mineralization associated with fluids whose origins lie in metamorphic devolatilization, but which may include examples where magmatic fluids are also a component (Goldfarb and Groves 2015). Further differences may be associated with generic geological systems dependent upon the age of mineralization, with Archaean and Proterozoic examples often exhibiting different auriferous mineral assemblages than their Phanerozoic counterparts (Chapman et al. 2009, 2021b).

Against this backdrop it is unsurprising that a wide variety of compositional signatures have been observed in gold mineralization categorized as 'orogenic'. Despite this complexity, our ability to characterize gold from orogenic environments is generally well advanced, primarily because of the close association of this style of mineralization with placer deposits and the resulting availability of samples. Consideration of economically important Precambrian gold mineralization have identified generic 'high fineness' (Goldfarb et al. 2005), but these authors acknowledged that gold from Phanerozoic systems may be more Ag rich. Wide variations in Ag content of gold according to locality may occur in a relatively small area, e.g. gold from hypogene and placer environments in the Eldorado Creek valley within a 5 km

radius of the Lone Star deposit, Klondike, Yukon, Canada (Chapman et al. 2010a) illustrated by six sample populations in Figure 4A. Gold from hypogene settings may show a narrow range in composition (Lone Star), or exhibit a range of Ag contents consistent with an evolving system where gold compositions reflect changes in P-T-X (Nugget Zone). Signatures of placer gold reflect that of their source(s). Gay Gulch drains the Lone Star Ridge, and the signature of the placer gold is a composite of such signatures. However, placer localities on the opposite side of the Edorado Creek yield gold with a far higher Ag content, more similar to that observed in occurrences such as the Violet Mine (Chapman et al. 2010a). Gold from Archaean orogenic mineralization generally shows a range of Ag contents at lower levels (e.g., gold from Kwekwe, Zimbabwe, Fig. 4A) and most examples of gold mineralization hosted in the granite-greenstone belts of west and east Africa exhibit detectable Cu (Omang et al. 2015; Dongmo et al. 2018; Chapman et al. 2021a).

Within the class of Phanerozoic orogenic gold occurrences, there appear to be generic signatures defined by the non-metal content. Sulphides are ubiquitous but As, Sb and Te may also be present singly or in combination (Fig 4B). These associations have also been observed in other examples worldwide (e.g., Chapman et al. 2000) which attests to their use as discriminants. Figures 4C-D provide examples of mineral inclusion species commonly encountered in gold from orogenic systems. These minerals may also be present as part of a more mineralogically complex inclusion suite in gold from magmatic hydrothermal systems. There are similarities between signatures of gold from some epithermal systems and some orogenic systems in that both exhibit a strong Ag-Te signature (compare radar diagrams for Klaza (Fig. 3G) and Eureka Creek and Adams/Skookum Creeks (Fig. 4B)). This inclusion signature may be a consequence of similar mineralizing environments in epizonal orogenic and epithermal mineralization. The hypothesis of a generic process of gold formation is consistent with similarities in both alloy and inclusion suites between gold from several localities in the Klondike, exemplified by gold from Adams and Eureka creeks (Fig. 4A).

Gold from most Archaean orogenic localities contains few inclusions, which precludes meaningful depiction in radar diagrams. Where present, the inclusion assemblage generally comprises pyrite, pyrrhotite (Fig. 4F) and chalcopyrite (Chapman et al. 2021b). Inclusions are more common in gold from Kwekwe in the greenstone belt of Zimbabwe (Naden et al. 1994) and the resulting radar diagram is shown in Fig. 4B. The signature is unlike any generated by populations of Phanerozoic orogenic gold because of the pronounced Bi-Te signature which, as discussed above, suggests the influence of igneous rocks on the fluid chemistry.

Gold formed in low temperature oxidizing chloride systems

Redox-driven precipitation of both uranium and copper mineralization is well known, and some systems may contain gold, such as the Polish Kupferscheifer (Piestryzinski et al. 2002) and Australian uranium deposits (Mernagh et al. 1994). The origins of various Brazilian Au-Pd deposits have also been ascribed to metal precipitation at redox boundaries (e.g., Olivo et al. 1995, Cabral et al. 2002). It seems likely that gold precipitation is commonly associated with redox interfaces between oxidizing and reducing lithologies but is probably under-reported as this environment is not generally regarded as prospective for gold. Furthermore,

the gold particles are commonly in the size range 50-500 μm , which can easily pass unnoticed if the field worker is not actively looking for small gold particles. Nevertheless, we have considered their composition here as they exhibit distinctive compositional features and hence could find application as an indicator mineral for other elements present in redox-controlled mineralization.

Gold formed in this environment exhibits a range of signatures associated with decreasing Eh during mineral precipitation (Chapman et al. 2009). Initially, Au alloy is nearly pure, (type i) and Pd is co-precipitated as Eh decreases (Fig. 5B) to generate a Au-Pd alloy (type ii). Thereafter, Ag-Au alloy (type iii) predominates. The Au-Pd ($\pm\text{Pt}$) association results from the co-mobility of these metals in oxidized chloride hydrothermal systems (Mountain and Wood 1988). Inclusion suites are commonly mineralogically complex (Fig. 5B), comprising selenides and tellurides of many metallic elements, plus various intermetallic compounds (Figs. 5 C, D). Three examples of inclusion radar diagrams are provided (Fig. 5B) relating to regional sample suites from localities adjacent to Devonian red beds in the Lammermuir Hills (Scotland), Permian red beds in Ayrshire (Scotland), and localities in Devon, (England). The dominance of selenides and tellurides is clear, together with a relatively complex metal signature. The shape of these radar plots is distinct from radar plots of gold formed in any other environment.

Consideration of individual sample suites reveals that the proportion of each alloy type varies considerably between localities within a region. Figures 5A and 5B show that the gold from Devon (a region of Permian red sandstones) and the Lammermuir Hills (a region of Devonian red sandstone) is very similar, but that the sample population from Ayrshire contains a higher proportion of gold type iii. The range of alloy profiles observed here is interpreted as indicative of locally different redox profiles during metal precipitation. Similarly, the inclusion suite may contain different metallic elements at different localities, reflecting the metal reservoirs in the adjacent oxidizing lithologies. Irrespective of the metal suite, selenides comprise the dominant mineral class and a range of intermetallic compounds are far more common than in gold from other deposit types (Fig. 5D).

The mechanism of Au precipitation at red bed margins is likely associated with high redox gradients. Whilst the gold particles are normally very small (typically 100-500 μm), their morphology may be distinctive. Gold precipitated in conditions of pronounced disequilibrium forms dendritic particles, whose habit changes to triangular forms with decreasing redox gradient (Sunagwa 1981). Dendritic particles are very common in all regions where this gold type occurs and some examples are illustrated in Figure 5E. The pristine crystal shapes are clearly indicative of very limited fluvial transport, but relict features may be observed in other particles which are relatively distal. High incidence of gold particles with these features has provided a clear indication of deposit type during sample collection.

Potential applications of gold as an indicator mineral

The majority of studies which have focussed on placer-lode relationships have been undertaken in the context of regional gold exploration (e.g. Potter and Styles 2003; Omang et

al. 2015; Lalomov et al. 2016; Alam et al. 2018; Nevolko et al. 2019). Such studies are a refinement of the classic ‘panning back to the source’ approach historically adopted by prospectors, because the variation between compositional signatures of sample populations provides a discriminant for different sources. Some studies benefitted from large sampling campaigns which provided sufficient data for interrogation (e.g. Leake et al. 1998, Chapman et al. 2000a). Subsequent work in other localities globally has permitted the identification of specific signatures diagnostic for gold from different source styles, as described above. These data sets provide a platform for interpreting new information from studies that have access to more modest data sets.

Detrital gold remains an excellent indicator for gold deposits, simply because of its presence in erosional products (McClenaghan and Cabri 2011), but the standard interpretations of particle size, morphology and abundance can be greatly aided by consideration of compositional criteria. Several local and regional studies of orogenic gold have revealed clearly distinct microchemical signatures either associated with several episodes of mineralization or zoning (Leake et al 1998; Chapman et al. 2000b; Chapman et al 2010a,b, Chapman and Mortensen 2016, Moles and Chapman 2019). Consideration of the relative prevalence of particular signatures of placer gold populations with signatures of gold from local lodes (Chapman et al. 2010a,b, Chapman and Mortensen 2016), together with placer mining records (Chapman and Mortensen 2016) can identify the signature(s) of the most economically important types.

Our understanding of the difference in signatures of gold formed in different deposit types could find application in several areas. Firstly, targeted studies in the Canadian Cordillera have demonstrated the utility of gold as an indicator mineral for Cu-Au (Mo) porphyry systems (Chapman et al. 2017, 2018). This development has only been possible because gold formed in these magmatic-hydrothermal systems may be distinguished from that formed in orogenic systems.

Secondly, redox controlled U-Au mineralization has been reported in Australia at Coronation Hill, (Mernagh et al. 1994) and in the Alligator Rivers uranium field (Wilde et al. 1989). In addition, Tremblay (1982) reported a U-Au association at several Canadian localities in Saskatchewan, particularly where mineralization occurred at unconformities. Davidson and Ghandi (1989) report an Au-Ag-Hg-Pd-Pt-Te-Se mineral and alloy association in the Boomerang Lake U-Au prospect in the Northwest Territories, Canada and note that similar associations have been observed at various other localities of uranium mineralization in Canada. As discussed above, gold alloy precipitated in low temperature-redox controlled systems has distinctive characteristics (Chapman et al. 2009) and the genetic association of U mineralization with gold exhibiting readily identifiable compositional characteristics provides a basis to utilize gold particles as a deposit-specific indicator.

Thirdly, the co-occurrence of gold and PGM derived from ultrabasic lithologies in placer deposits has been reported in many districts worldwide but there is not always a genetic relationship. Compositional studies of both gold and PGMs can indicate an association (Fig. 5, and Zaykov et al. 2017; Barkov et al. 2018) or absence of an association (Svetlistkays et al.

2018). Gold genetically related to PGM may show distinctive characteristics such as those illustrated in Figures 3K-M. The exsolution of auricupride (AuCu) from Cu-rich Au-Ag alloy indicates an original high formation temperature permissive of elevated levels of Cu. This microfabric is associated with copper sulphide inclusions (Fig. 3L) which deviate from the stoichiometric ideal due to the presence of small amounts of Fe (Chapman: unpublished data). The intimate Au-PGE association recorded in gold from southern Namibia (Fig. 3M) also underlines how mineralogical studies of placer gold can establish genetic relationships indicative of a deposit type. This information is clearly critical during proposal of deposit models and associated exploration strategies.

Future developments

Analytical approaches

The application of ToF LA-ICP-MS (hereafter ToF-MS) systems to the characterization of gold alloy provides the opportunity gain both compositional and textural information at the trace and ultra-trace levels (Banks et al. 2018, Chapman et al. 2021a). The elemental maps generated permit spatial evaluation of trace element heterogeneity and co-variance. This information may also be inferred from the study of large numbers of gold particles using a quadrupole MS system, in a similar fashion to the approach routinely employed to interpret compositional variation in data sets generated by EPMA and SEM screening of inclusions. The adoption of a methodology involving analysis using a ToF-MS system could provide a more efficient route to characterization of a sample population, but methodologies to convert spatial information on element concentration and distribution to a data format that permits comparison of sample populations have yet to be developed. Currently, widespread adoption of the ToF-MS analytical methodology is compromised both by limited access to facilities and the time investment by operators to generate the output for interpretation. It remains the case that sufficient gold particles should be studied to adequately characterize a population in which compositional heterogeneity is common both within and between particles. Ultimately, a dual approach using screening by EPMA followed by ToF-MS of selected particles may prove optimal.

The degree of heterogeneity within gold particles revealed by ToF LA-ICP-MS has implications for the approach to particle characterization using a quadrupole LA-ICP-MS system. Chapman et al. (2021b) considered the effect of laser spot sampling on elemental response in the context of the distribution of elements at a polished particle surface as revealed by TOF LA-ICP-MS analysis and it is clear that the analysis values would be highly dependent upon spot location. There is no visual guide to laser spot positioning available to the operator, because the target appears homogenous, both in BSE and optical imaging. Nevertheless, the nature of trace element heterogeneity in gold revealed by ToF-MS analysis greatly informs our ability to interpret data derived from quadrupole systems in terms of the causes of elemental responses, and to critique published data sets in terms of the number of particles analysed.

Practical considerations

The issues surrounding collection of gold particles have been discussed in relation to logistical considerations (Moles and Chapman 2019) and the requirement to generate robust data sets (Chapman et al. 2021b). Several factors may act to undermine the suitability of the approach in a particular area. Gold particles of less than around 50 μm do not exhibit markedly different hydrodynamic behaviour from their sand/gravel sized sediment matrix, so they neither accumulate in specific fluvial environments nor are they easily collectable by standard field gravity separation techniques. Progressive transport of gold particles results in deformation of the gold such that inclusions may be obliterated through contact with oxidizing surficial environments. The net effect is the reduction in inclusion abundance with transport distance (Loen 1995, Melchiorre and Henderson 2019) and consequently collection of samples distant from the source generally requires more gold particles to characterize the inclusion suite.

Such long transport distances also increase the potential for gold from various sources to be mixed within a single population of placer particles, and in areas where continental glaciation has been prevalent, there is a potential for transportation of gold particles between valley catchments. However, in areas of valley glaciation, the signatures of gold from adjacent drainages are often clearly distinguishable (e.g. Leake et al. 1998, Moles and Chapman 2019). Studies that have successfully resolved regional variation in gold signatures have, wherever possible, sampled multiple tributaries with smaller catchment areas rather than relying on collection of gold from trunk drainages (e.g. Chapman et al. 2010a,b, Chapman and Mortensen 2016).

Characterization of inclusion suites may necessitate relatively large sample populations comprising c 250 particles, and alternative approaches that require smaller numbers would clearly be advantageous, especially in scenarios where inclusions are scarce. Unfortunately, this aspiration is unlikely to be fulfilled by the adoption of methodologies based on quadrupole MS systems because of the intra- and inter-gold particle heterogeneity at trace levels, discussed above.

Consequently, the main barrier to the effective use of gold as an indicator mineral remains the need to collect sufficient material for analysis. To some extent, these issues may be mitigated using new approaches to data analysis, and these are discussed below.

Application of multivariate statistical analysis to large data sets

Interpretation of compositional data sets describing sample populations of gold particles presents several challenges. The wide range of compositional signatures observed in gold from different geological settings globally are represented in diverse literature and, for researchers new to the subject, interpretation of new data sets demands a level of familiarity with previous work that may be unrealistic. One approach to alleviating the need for specialist knowledge is the application of statistical methods to provide mathematically derived characterisations according to multivariate discriminants. Interrogation of data sets by principle component analysis (PCA) has found application in geochemical exploration where large numbers of sample locations are characterized by multi-element data (e.g.

Ghezelbash et al. 2019, Zuo 2011, Zuo et al. 2016). There is a clear parallel between the challenges faced by these studies and those involving interpretation of compositional data for sample populations of gold particles.

Previous gold compositional studies have established specific characteristics that are indicative of the source style of mineralization, e.g., the Pb-Bi-Te-S inclusion suite associated with calc-alkalic porphyry systems (Chapman et al. 2018). Such signatures would be evident in principle components derived from the raw data set. Consequently, it should be possible to generate discriminatory diagrams which define compositional ranges of gold associated with different classes of ore deposit. Once established, the resulting templates could be used to identify the nature of 'unknowns' resulting from ongoing exploration.

Liu et al. (2021) used EMP and quadrupole LA-ICP-MS to analyse a total of 287 gold grains within hypogene ore samples from orogenic gold deposits in order to investigate the influences of paragenetic stage and host lithology on gold composition. They subjected their log-ratio transformed chemical data to partial least-squares discriminant analysis (PLS-DA) and reported differing signatures in terms of Ag, Cu, Pd, Sb and Hg according to local lithologies. Focussed and well-constrained studies such as this provide a route to evaluate fluid-rock interaction and illuminate depositional processes. In addition, the study highlighted the potential of detrital gold particle trace element analysis to identify host lithologies of the source, which could be particularly valuable in regions comprising metasediment lithologies.

The following section describes a pilot study in which our own data have been rigorously interrogated to create a classification algorithm that replicates the manual approach to data interpretation. The data used in this section comprise LA-ICP-MS analyses describing 35 elements of 656 gold particles collected from 27 localities, previously described by Banks et al. (2018).

In many cases, elements were present below the detection limit (DL). In the event of values <DL, a zero was reported in the database; any zeroes were converted to $\frac{1}{2}$ the lowest real value in the dataset for each individual element. A few elements (Ge, Se, Al, Ti, and Y) were not considered in the interpretation because they had too few non-censored values. The remaining 30 elements were subjected to further interpretation using multivariate analysis to assess variable importance. A linear discriminant function (LDF) identified which of the 30 variables was the most useful for separating these *a priori* groupings (orogenic, LS epithermal, and alkalic porphyry). The variable importance was measured using Wilks' Lambda (Λ), which is expressed as the ratio of the determinants of \mathbf{W} to $\mathbf{B}+\mathbf{W}$ (Tatsuoka 1988) where \mathbf{W} is the within-group distance and \mathbf{B} is the between-group distance. The following variables were selected for further interpretation and incorporation to the classification schema: As, Au, Cd, Co, Cr, Cu, Fe, Hg, Pb, Pd, Te, V, W, and Zn. The elements with the lowest Wilks Λ (therefore the most important variables for group separation) are Cu, Hg, Pb, Pd, Sn, Co, Rh, and Au. The classification tree (Supplementary Data) shows Au, Cu, and Hg as the nodes near the top of the tree, meaning they have the most importance for deposit type discrimination.

The data set available to the study is imbalanced i.e. there are different numbers of gold particles relating to each of the deposit types (alkalic porphyry: $n = 260$, orogenic: $n = 330$, and LS epithermal: $n = 20$). The challenge of working with imbalanced datasets is that most machine learning techniques will ignore, and in turn have poor performance on, the minority class, although typically it is performance on the minority class that is most important. Compositional studies such as this commonly involve comparative interrogation of data sets of different sizes, and as in this case it may be necessary to manipulate data prior to analysis. There are two main workflows to circumvent class imbalance: under-sampling the majority class, in this case analyses relating to gold from orogenic and alkalic porphyry mineralization, or over-sampling the minority class, in this case LS epithermal. The simplest approach to handling imbalanced datasets involves duplicating examples in the minority class, however a more robust approach is to synthesize new data from existing data. This is called data augmentation, or Synthetic Minority Oversampling Technique (SMOTE), and it works by selecting examples that are close in the feature space, drawing a line between the examples in the feature space and creating a new sample at a point along that line (Chawla et al. 2002). An example of the synthetic oversampling results is shown in the probability plot of Cu data (Fig. 6), where all blue datapoints (synthetic) can be observed within the bounds of the natural data points (red).

Several machine learning classification models were tested and evaluated, using 10-fold cross validation and stratified sampling, and the model evaluation results are listed in Table 2. The highest Classification Accuracy (CA) was obtained using the random forest, and this approach is discussed in more detail below.

Random forests are a combination of tree predictors such that each tree depends on the values of a random vector sampled independently and with the same distribution for all trees in the forest (Breiman 2001). For gold compositional data this equates to applying randomly selected criteria (chemical elements) to the data set. A random forest Machine Learning model was used to create a multiclass classification scheme, using supervised training data (deposit type). Data were classified and split according to a criterion which generates the clearest demarcation of the deposit type data and the resulting subsets were treated in a similar manner in the second stage of an iterative approach. The process was repeated, generating a decision tree with nodes defined by concentration of a specific element. The decision tree flowing from this exercise is a physically large diagram, which cannot be adequately depicted on a journal page. Consequently it is included as supplementary material.

For the sample suite used here, the most important element to differentiate gold from LS epithermal environments and from orogenic settings is Au, but this is a data set specific result related to the high Ag values in gold particles from Black Dome, which dominate the LS epithermal sample set. Classification is also influenced by Cu, Hg, and As. The most important element to differentiate gold from alkalic porphyry deposits from orogenic gold is Cu, followed by Co. The full figure in the supplementary data shows the details of elemental breaks and ranges associated with each deposit type.

The data set available to the study is relatively small and some data sets relate to gold particles from a limited number of localities. Therefore, the following classification serves to

illustrate a methodology, rather than to make any claims regarding generic compositional characteristics. Future work drawing upon larger data sets will clarify these generic relationships.

The size of diagram required to adequately illustrate decision trees has encouraged design of alternative visual methods. A Pythagorean forest is a group of Pythagoras trees that can be used to visualize hierarchical classifications; the fractal approach is named after Pythagoras because every branch creates a right triangle and the Pythagorean theorem is applicable to the areas of the squares (Beck 2014). Other metrics are incorporated into the tree in terms of segment size and branching angles, and the resulting figure is easier to assimilate than a series of complex decision trees. Figure 7 shows a Pythagorean tree corresponding to the decision tree shown in the Supplementary Information. The areas specific to each deposit style are clearly visible.

Conclusions

Native gold particles exhibit a range of compositional characteristics as a result of different mineralizing environments. Consequently, gold formed in different styles of gold mineralization may be recognised according to combinations of alloy chemistry and the suite of mineral inclusions preserved within the particles. Whilst not all signatures are mutually exclusive, there are sufficient generic differences to permit compositional characterization of gold according to source style. These compositional features are inherited by detrital gold particles, thereby providing a basis for a source-specific indicator mineral methodology.

Recent advances in understanding the heterogeneity of gold particles and the availability of large data bases of gold compositions have implications for the design of individual studies. On a practical level it is necessary to characterize an adequate number of gold particles to characterize a population. Mineral inclusions are the most powerful discriminants but their apparent scarcity is problematic where only small sample sets are available. Similarly, sufficient particles are required to characterize sample populations using quadrupole-MS analysis in conjunction with LA-ICP systems, because of the potential of heterogeneity in the ablation target to generate a highly spurious value. Nevertheless, generic compositional templates have been developed describing gold from a wide range of orogenic, porphyry, epithermal and redox-controlled mineralization, and compositional templates will improve as more quantitative data describing minor elements such as Cu, Hg and Pd becomes available from studies using LA-ICP-MS. As gold may be an accessory mineral in deposit types such as porphyry Au-Cu, redox controlled U deposits, or magmatic/magmatic-hydrothermal Au-PGE mineralization, its potential as an indicator extends beyond exploration for gold-only deposits, and furthermore, the signatures of gold from these deposit types is distinctive.

The application of Exploratory Data Analysis to large data sets describing gold compositions show that Random forests are superior in discriminating compositional ranges based on the elements detected using LA-ICP-MS. Depiction of outcomes using a Pythagorean forest provides a convenient 2D graphical mechanism to visualise the multivariate data. Synthesis

of new approaches to data interrogation coupled with robust data sets flowing from an understanding of compositional nature of gold will facilitate future developments.

Acknowledgements

We would like to thank Dr Beth McClenaghan and an anonymous reviewer for their thorough reviewing of the manuscript and for many useful suggestions which improved the quality of the final submission.

ACCEPTED MANUSCRIPT

References

- ALAM, M., LI, S.R., SANTOSH, M., & YUAN, M.W. 2018. Morphology and chemistry of placer gold in the Bagrote and Dainter streams, northern Pakistan: implications for provenance and exploration. *Geological Journal*, **54**, 1672-87.
- ANTWEILER, J.C., & CAMPBELL, W. 1977. Application of gold compositional analyses to mineral exploration in the United States. *Journal of Geochemical Exploration*, **8**, 17-29.
- AVERILL, S. A. 2001. The application of heavy indicator mineralogy in mineral exploration with emphasis on base metal indicators in glaciated metamorphic and plutonic terrains. *Geological Society, London, Special Publications*, **185**, 69-81.
- AVERILL, S.A. 2017. The Blackwater gold-spessartine-pyrolusite glacial dispersal train, British Columbia, Canada; influence of sampling depth on indicator mineralogy and geochemistry. *Geochemistry: Exploration, Environment, Analysis*, **17**, 43- 60.
- BANKS, D.A., CHAPMAN, R.J. & SPENCE-JONES, C.P. 2018. Detrital gold as a deposit-specific indicator mineral by LA-ICP-MS analysis. *Geoscience BC report 2018-21*. Available at: <http://www.geosciencebc.com/s/2016-006.asp>
- BARKOV, A.Y., SHVEDOV, G.I., SILYANOV, S.A. AND MARTIN, R.F., 2018. Mineralogy of platinum-group elements and gold in the ophiolite-related placer of the river Bolshoy Khailyk, western Sayans, Russia. *Minerals*, **R** 247-271.
- BARNETT, P.J. & AVERILL, S. 2010. Heavy mineral dispersal trains in till in the area of the Lac des Iles PGE deposit, northwestern Ontario, Canada. *Geochemistry: Exploration, Environment, Analysis*, **10**, 391-399.
- BECK, F., BURCH, M., MUNZ, T., DI SILVESTRO, L. & WEISKOPF, D. 2014. Generalized Pythagoras Trees for Visualizing Hierarchies. In IVAPP '14 Proceedings of the 5th International Conference on Information Visualization Theory and Applications, 17-28.
- BONEV, I. K., KERESTEDJANT, A. R., & ANDREW, C. J. 2002. Morphogenesis and composition of native gold in the Chelopech volcanic –hosted Au-Cu epithermal deposit Srednorgorie zone, Bulgaria. *Mineralium Deposita*, **37**, 614-629.
- BOUZARI, F., HART, C.J.R., BARKER, S. & BISSIG, T. 2010. Porphyry indicator minerals (pims): exploration for concealed deposits in south central British Columbia (NTS 092I/06, 093A/12, 093N/01, /14); *IN Geoscience BC Summary Of Activities 2009, Geoscience BC, Report 2010-1*, 25–32.
- BOUZARI, F., HART, C.J.R., & BARKER, S. 2016. Hydrothermal alteration revealed by apatite luminescence and chemistry: a potential indicator mineral for exploring covered porphyry copper deposits. *Economic Geology*, **111**, 1397–1410.
- BOYLE RW (1979) the geochemistry of gold and its deposits. *Geological Survey of Canada Bulletin*, 280p.
- BREIMAN, L. (2001). Random forests. *Machine Learning*, 45(1), 5-32
- CELIS, M.A., BOUZARI, F., BISSIG, T., HART, C.J.R. & FERBEY, T. 2014. Petrographic characteristics of porphyry indicator minerals from alkalic porphyry copper-gold deposits in south-central British Columbia (NTS 092, 093); *In Geoscience BC Summary Of Activities 2013, Geoscience BC, Report 2014-1*, 53–62.
- CABRAL, A.R., LEHMANN, B., KWITCO, R., & CRAVO COSTA, C.H. 2002. The Serra Pelada Au-Pd-Pt deposit Carajás mineral province northern Brazil: reconnaissance mineralogy and chemistry of very high grade palladiferous gold mineralization. *Economic Geology*, **97**, 1127-1138.
- CHAWLA, N.V., BOWYER, K.W., HALL, L.O., KEGELMEYER, W.P. 2002.

- Smote: synthetic minority over-sampling technique. *J. Artif. Intell. Res.* 16, 321-357.
- CHAPMAN, J.B., PLOUFFE, A., AND FERBEY, T., 2015. Tourmaline: the universal indicator?; 27th international applied geochemistry symposium, tucson, az, application of indicator mineral methods to exploration, short course no. 2, 25-31.
- CHAPMAN, R. J. & MORTENSEN, J. K. 2006. Application of microchemical characterization of placer gold grains to exploration for epithermal gold mineralization in regions of poor exposure. *Journal of Geochemical Exploration*, **91**, 1–26.
- CHAPMAN, R.J., & MORTENSEN, J.K. 2016 Characterization Of Gold Mineralization In The Northern Cariboo Gold District, British Columbia, Canada, Through Integration Of Compositional Studies Of Lode And Detrital Gold With Historical Placer Production: A Template For Evaluation Of Orogenic Gold Districts. *Econ Geol* 111:1321-1345. Doi: 10.2113/Econgeo.111.6.1321.
- CHAPMAN, R. J., LEAKE, R. C., MOLES, N. R., EARLS, G., COOPER, C., HARRINGTON, K. & BERZINS, R. 2000a. The application of microchemical analysis of gold grains to the understanding of complex local and regional gold mineralization: a case study in Ireland and Scotland. *Economic Geology*, **95**, 1753–1773.
- CHAPMAN, R.J., LEAKE, R.C. & FLOYD, J. 2000b Gold mineralization in the vicinity of Glengaber Burn, Scottish Borders. *Scottish J Geol* **36**: 165-176.
- CHAPMAN, R.J., SHAW, M., LEAKE, R.C. & JACKSON B 2005 Gold mineralisation in the central Ochil Hills, Perthshire, UK. *T I Min Metall B Appl Earth Sci* **114**:53-64.
- CHAPMAN, R.J., LEAKE, R.C., WARNER, R.A., CAHILL, M.C., MOLES, N.R., SHEL, L C.A. & TAYLOR J.J. 2006 Microchemical characterisation of natural gold and artefact gold as a tool for provenancing prehistoric gold artefacts: A case study in Ireland. *Appl Geochem* **21**: 904-918.
- CHAPMAN, R. J., LEAKE, R. C., BOND, D. P. G., STEDRA, V. & FAIRGRIEVE, B. 2009. Chemical and mineralogical signatures of gold formed in oxidizing chloride hydrothermal systems and their significance within populations of placer gold grains collected during reconnaissance. *Economic Geology*, **104**, 563–585.
- CHAPMAN, R. J., MORTENSEN, J. K., CRAWFORD, E. C. & LEBARGE, W. 2010a. Microchemical studies of placer and lode gold in the Klondike District, Yukon, Canada: 2. Constraints on the nature and location of regional lode sources. *Economic Geology*, **105**, 1369–1392.
- CHAPMAN, R. J., MORTENSEN, J. K., CRAWFORD, E. C. & LEBARGE, W. 2010b. Microchemical studies of placer and lode gold in Bonanza and Eldorado creeks, Klondike District, Yukon, Canada: evidence for a small, gold-rich, orogenic hydrothermal system. *Economic Geology*, **105**, 1393–1410.
- CHAPMAN, R.J., MORTENSEN, J.K. & LEBARGE, W.P. 2011 Styles of lode gold mineralization contributing to the placers of the Indian River and Black Hills Creek, Yukon Territory, Canada as deduced from microchemical characterization of placer gold grains. *Miner Deposita* **46**:881-903.
- CHAPMAN R.J., MILEHAM, T.J., ALLAN, M.M., & MORTENSEN, J.K. 2017. A distinctive Pd-Hg signature in detrital gold derived from alkalic Cu-Au porphyry systems. *Ore Geology Reviews* **83**, 84-102.
- CHAPMAN, R.J., ALLAN, M.M., MORTENSEN, J.K., WRIGHTON, T.M. & GRIMSHAW, M.R. 2018. A new indicator mineral methodology based on a generic Bi-Pb-Te-S mineral inclusion signature in detrital gold from porphyry and low/intermediate sulfidation epithermal environments in Yukon Territory, Canada. *Mineralium Deposita* **53**, 815-834.
- CHAPMAN, R.J., CRAW, D., MOLES, N.R. & WALSHAW, R.D. 2021a Evaluation of the contributions of gold derived from hypogene, supergene and surficial processes in the

- formation of placer gold deposits. GSL Special publication: From orogeny to Alluvium. (Torvela, Chapman and Lambert-Smith Eds).
- CHAPMAN, R.J., BANKS, D.A., STYLES, M.T., WALSHAW, R.D., PIAZOLO, S., MORGAN, D.J., GRIMSHAW, M.R., SPENCE-JONES, C.P., MATTHEWS, T.J., & BOROVINSKAYA, O. 2021b Chemical and physical heterogeneity within native gold: implications for the design of gold particle studies. *Mineralium Deposita* <https://doi.org/10.1007/s00126-020-01036-x>
- CHAPMAN, .R.J., MORTENSEN, J.K, ALLAN, M.M., WALSHAW, R.D., BOND, J. & MACWILLIAM, K. In Press. A new approach to characterizing deposit type using mineral inclusion assemblages in gold particles. *Economic Geology*
- CHUDNENKO, K.V. & PALYANOVA, G.A. 2016 Thermodynamic modeling of native formation of Au–Ag–Cu–Hg solid solutions: *Applied Geochemistry*, **66**, 88-100.
- COOKE, D.R., AGNEW, P., HOLLINGS, P., BAKER, M., CHANG, Z., WILKINSON, J.J., WHITE, N.C., ZHANG, L., THOMPSON, J., GEMMELL, J.B., FOX, N., CHEN, H., & WILKINSON, C.C., 2017. Porphyry indicator minerals (PIMS) and porphyry vectoring and fertility tools (PVFTS) – indicators of mineralization styles and recorders of hypogene geochemical dispersion haloes; *in* Proceedings of Exploration 17: Sixth Decennial International Conference on Mineral Exploration, (eds.) V. Tschirhart and M.D. Thomas; 457–470.
- CRAW, D., & KERR, G. 2017. Geochemistry and mineralogy of contrasting supergene gold alteration zones, southern New Zealand. *Applied Geochemistry*, **85**, 19-34.
- DAVIDSON, G.I. & GANDHI, S.S. 1989. Unconformity-related U-Au mineralization in the middle Proterozoic Thelon sandstone, Boomerang Lake Prospect, Northwest Territories, Canada. *Economic Geology*, **84**, 143-157.
- DONGMO, F.W.N., CHAPMAN, R.J., BOLARINWA, A.T., YONGUE, R.F, BANKS, D.A, & OLAJIDE-KAYODE, J.O. 2018. Microchemical characterization of placer gold grains from the Meyos-Essabikoula area, Ntem complex, southern Cameroon. *Journal of African Earth Science* **151**:189-201.
- DUNN, S.C., BJORN, P., ROZENDAAL, A. & TALJAARD, R. 2019. Secondary gold mineralization in the Amani Placer Gold Deposit, Tanzania. *Ore Geology Reviews*, **107**, 87-107.
- FISHER, N.H. 1945. The fineness of gold, with special reference to the Morobe gold field, New Guinea. *Economic Geology*, **40**, 449-495.
- GAMMONS, C. H. & WILLIAMS-JONES, A. E. 1995. Hydrothermal geochemistry of electrum: Thermodynamic constraints: *Economic Geology*, **90**, 420-432.
- GHEZELBASH, R., MAGHSOUDI, A., CARRANZA, E.J. 2019 Mapping of single-and multi-element geochemical indicators based on catchment basin analysis: Application of fractal method and unsupervised clustering models. *Journal of Geochemical Exploration*. **199**, 90-104.
- GIRARD, R., TREMBLAY, J., NÉRON, A., LONGUEPÉE, H., & MAKVANDI, S. 2021. Automated gold grain counting, Part 2: What a gold grain size and shape can tell! *Minerals*, **11**, 379.
- GOLDFARB, R.J., BAKER, T., DUBÉ, B., GROVES, D.I., HART, C.J.R. & GOSSELIN, P. 2005. Distribution, character and genesis of gold deposits in metamorphic terranes; in HEDENQUIST, J. W., THOMPSON, J.F.H., GOLDFARB, R.J. AND RICHARDS, J.P., EDS., *Economic Geology 100th Anniversary Volume*, 407-450.
- GOLDFARB, R.J. & GROVES, D.I. 2015. Orogenic gold: common or evolving fluid and metal sources through time. *Lithos*, **233**, 2-26.
- GROEN, J. C., CRAIG, J. R. & RIMSTIDT, J. D. 1990. Gold-rich rim formation on electrum grains in placers. *Canadian Mineralogist*, **28**, 207–228.

- HENNEY, P.J., STYLES, M.T., BLAND, D.J. & WETTON, P.D. 1994 Characterization of gold from the Lubuk Mandi area, Terengganu, Malaysia: British Geological Survey, Technical Report WC/94/21, 28 p
- HOUGH, R. M., BUTT, C. R. M. & FISCHER-BUHNER, J. 2009. The crystallography, metallography and composition of gold. *Elements*, **5**, 297-302.
- KNIGHT, J.B. & LEITCH, C.H. 2001 Phase relations in the system Au–Cu–Ag at low temperatures, based on natural assemblages. *The Canadian Mineralogist*, **39**:889-905.
- KNIGHT, J. B., MORTENSEN, J. K., AND MORISON, S. R. 1999a. Lode and placer gold composition in the Klondike district, Yukon Territory, Canada: Implications for the nature and genesis of Klondike placer and lode gold deposits: *Economic Geology*, **94**, 649–664.
- KNIGHT, J. B., MORISON, S. R. & MORTENSEN, J. K. 1999b. The relationship between placer gold particle shape, rimming and distance of fluvial transport; as exemplified by gold from the Klondike District, Yukon Territory, Canada. *Economic Geology*, **94**, 635–648.
- LALOMOV, A.V., CHEFRANOV, R.M., NAUMOV, V.A., NAUMOVA, O.B., LEBARGE, W. & DILLY, R.A. 2016. Typomorphic features of placer gold of Vagran cluster (the Northern Urals) and search indicators for primary bedrock gold deposits, *Ore Geology Reviews* **85**, 321-35. <http://dx.doi.org/10.1016/j.oregeorev.2016.06.018>
- LEAKE, R.C., BLAND, D.J., STYLES, M.T. 1991. Internal structure of Au-Pd-Pt grains from south Devon, England, in relation to low-temperature transport and deposition. *Transactions of the Institution of Mining and Metallurgy, Section B*, **100**, 159-178.
- LEAKE, R. C., BLAND, D. J. & COOPER, C. 1992. Source characterization of alluvial gold from mineral inclusions and internal compositional variation. *Transactions of the Institution of Mining and Metallurgy (Section B Applied Earth Sciences)*, **102**, B65–82.
- LEAKE, R. C., CHAPMAN, R. J., BLAND, D. J., STONE, P., CAMERON, D. G. & STYLES, M. T. 1998. The origin of alluvial gold in the Leadhills area of Scotland; evidence from internal chemical characteristics. *Journal of Geochemical Exploration*, **63**, 7–36.
- LEAL, S. LIMA, A. & NORONHA, F. In press. Characterization of heavy mineral concentrates and detrital gold particles from the Bigorne granite-hosted gold deposit in the Iberian Variscan Belt. *GSL Special publication: From orogeny to Alluvium*. (Torvela, Chapman and Lambert-Smith, Eds)
- LIU, H., BEAUDOIN, G., MAKVANDI, S. JACKSON, S.E. & HUANG, X. 2021. Multivariate statistical analysis of trace element compositions of native gold from orogenic gold deposits: implication for mineral exploration, *Ore Geology Reviews* doi: <https://doi.org/10.1016/j.oregeorev.2021.104061>
- LOEN J.S. 1994. Origin of placer gold nuggets and history of formation of glacial gold placers, Gold Creek, Granite County, Montana. *Economic Geology* **89**, 91-104.
- LOEN, J.S. 1995. Use of placer gold characteristics to locate bedrock gold mineralization. *Exploration and Mining Geology*, **4**: 335–339.
- MAO, M., RUKHLOV, A.S., ROWINS, S.M., SPENCE, J. & COOGAN, L.A., 2016. Apatite trace element compositions: a robust new tool for mineral exploration. *Economic Geology*, **111**, 1187-1222.
- MANÉGLIA, N., BEAUDOIN, G. & SIMARD, M. 2018. Indicator Minerals Of The Meliadine Orogenic Gold Deposits, Nunavut (Canada), And Application To Till Surveys. *Geochemistry: Exploration, Environment, Analysis*, **18**, 241-251.
- MCCLENAGHAN, M.B., & KJARSGAARD, B.A. 2007. Indicator mineral and surficial geochemical exploration methods for kimberlite in glaciated terrain: Examples from Canada. In: W.D. Goodfellow (Ed.), *Mineral Deposits of Canada: A Synthesis of Major Deposit-Types, District Metallogeny, the Evolution of Geological Provinces, and Exploration Methods*.

- Geological Association of Canada, Mineral Deposits Division, Special Publication No. 5, pp. 983-1006.
- McCLENAGHAN, M.B., & LEIGHTON-MATTHEWS, D. 2017 Application of Mineral methods to bedrock sediments. *Application of indicator Minerals to Bedrock Sediments. Geological Survey of Canada Open File 8345*, ii.
- McCLENAGHAN, M.B. & CABRI, L.J. 2011. Review of gold and platinum group element (PGE) indicator minerals methods for surficial sediment sampling. *Geochemistry: Exploration, Environment, Analysis*, **11**, 251–263.
- McCLENAGHAN, M.B. AND PAULEN, R.C. Mineral Exploration in Glaciated Terrain; in Past Glacial Environments (Sediments, Forms and Techniques) A new & revised edition, (ed.) J. Menzies and J.J-M. van der Meer; Elsevier, 689-751.
- McCLENAGHAN, M.B., PAULEN, R.C., LAYTON-MATTHEWS, D., HICKEN, A.K., AND AVERILL, S.A. 2015b. Glacial dispersal of gahnite from the Izok Lake Zn-Cu-Pb-Ag VMS deposit, northern Canada. *Geochemistry: Exploration, Environment, Analysis*, **15**, 333-349.
- MELCHIORRE, E. B. & HENDERSON, J. 2019. Topographic gradients and lode gold sourcing recorded by placer gold morphology, geochemistry, and mineral inclusions in the east fork San Gabriel River, California, USA. *Ore Geology Reviews*, **109**, 348-357.
- MERNAGH, T.P., HEINRICH, C.A., LECKIE, J.F., CARVILLE, D.P., GILBERT, D.J., VALENTA, R.K. & WYBORN, L.A.I. 1994. Chemistry of low temperature hydrothermal gold, platinum and palladium (\pm uranium) mineralization at Coronation Hill, Northern Territory Australia. *Economic Geology* **89**, 1053-1073
- MOLES, N. R. & CHAPMAN, R. J. 2019. Integration of detrital gold microchemistry, heavy mineral distribution and sediment geochemistry to clarify regional metallogeny in glaciated terrains: application in the Caledonides of southeast Ireland. *Economic Geology*, **114**, 207-232.
- MOLES, N. R., CHAPMAN, R. J. & WARNER, R. B. 2013. The significance of copper concentrations in natural gold alloy for reconnaissance exploration and understanding gold-depositing hydrothermal systems. *Geochemistry: Exploration, Environment, Analysis*, **12**, 115-130.
- MORRISON, G. W., ROSE, W. J. & JAIRETH, S. 1991. Geological and geochemical controls on the silver content (fineness) of gold in gold–silver deposits. *Ore Geology Reviews*, **6**, 333–364.
- MORTENSEN, J.K, CRAW, D & MCKENZIE, D. (Submitted) Concepts and Revised Models for Phanerozoic Orogenic Gold Deposits. GSL Special publication: From Orogeny to Alluvium. (Torvela, Chapman and Lambert-Smith Eds)
- MOUNTAIN, B.W. & WOOD, S.A. 1988 Chemical controls on the solubility, transport and deposition of platinum and palladium in hydrothermal solutions: a thermodynamic approach. *Economic Geology*, **83**, 492-510.
- NADEN, J., STYLES, M.T. & HENNEY, P.J. 1994. Characterization of gold from Zimbabwe: Part 1. Bedrock gold: *British Geological Survey Technical Report WC/94/51*, 100p.
- NADEN, J. & HENNEY, P.J. 1995 Characterisation of gold from Fiji. *British Geological Survey Technical Report WC/95/41*, 31p
- NEVOLKO, P.A., KOLPAKOV, V.V., NESTERENKO, G.G. & FOMINYKH, P.A. 2019 Alluvial placer gold of the Egor’evsk District (Northern-Western Salair): composition characteristics, types and mineral microinclusions. *Russian Geology and Geophysics* **60**, 67-85.
- OLIVO, G.M., GAUTHIER, M., & BARDOUX, M. 1995. Palladium-bearing gold deposit hosted by Proterozoic Lake superior type Iron Formation at the Cauê iron mine, Itabira

- District, southern Sao Fransisco Craton, Brazil: geologic and structural controls. *Economic Geology* **90**, 118-134.
- OMANG, B.O., SUH, C.E., LEHMANN, B., VISHITI, A., CHOMBONG, NN., FON, A.N., EGBE, J.A. & SHEMANG, E.M. 2015. Microchemical signature of alluvial gold from two contrasting terrains in Cameroon. *Journal of African Earth Science* **112**,1-4.
- PIESTRYZINSKI, A., PIECZONKA, J., & GLUSEK, A. 2002. Redbed –Type Gold Mineralization, Kupferscheifer, South West Poland. *Mineralium Deposita* **37**, 512-528
- PISIAK, L.K., CANIL, D., LACOURSE, T., PLOUFFE, A. & FERBEY, T., 2017. Magnetite as an indicator mineral in the exploration of porphyry deposits: a case study in till near the Mount Polley Cu-Au deposit, British Columbia, Canada; *Economic Geology*, **112**, 919-940.
- PLOUFFE, A. & FERBEY, T., 2017. Porphyry Cu indicator minerals in till: A method to discover buried mineralization; *in* Indicator Minerals in Till and Stream Sediments of the Canadian Cordillera, (ed.) T. Ferbey, A. Plouffe, and A. Hickin; Mineral Association of Canada, Topics in Mineral Sciences Volume 47, Geological Association of Canada, Special Paper 50, 129-159.
- PLOUFFE, A., FERBEY, T., HASHMI, S., & WARD, B.C., 2016. Till geochemistry and mineralogy: vectoring towards Cu porphyry deposits in British Columbia, Canada; *Geochemistry: Exploration, Environment, Analysis*, **16**, 213-232.
- POTTER, M. & STYLES, M.T. 2003. Gold characterization as a guide to bedrock sources for the Estero Hondo alluvial gold mine, western Ecuador: *Transactions of the Institution of Mining and Metallurgy (Section B, Applied Earth Sciences)*, **112**, 297-304.
- REITH, F., REA, M.A., SAWLEY, P., ZAMMIT, C.M., NOLZE, G., REITH, T., RANTANEN, K., BISSETT, A. 2018. Biogeochemical cycling of gold: Transforming gold particles from arctic Finland. *Chemical Geology*, **483**, 511-29.
- STEWART, J., KERR, G., PRIOR, D., HALFPENNY, A., PEARCE, M., HOUGH R., & CRAW, D. 2017. Low temperature recrystallisation of alluvial gold in paleoplacer deposits. *Ore Geology Reviews*, **88**, 43-56.
- SUNAGWA, I. 1981. Characteristics of crystal growth in nature as seen from the morphology of mineral crystals: *Bulletin Minéralogie*, v. 104, p. 81-87.
- SVETLITSKAYA, T.V., NEVOLKO, P.A., KOLPAKOV, V.V. & TOLSTYKH, N.D. 2018 Native gold from the Inagli Pt–Au placer deposit (the Aldan Shield, Russia): geochemical characteristics and implications for possible bedrock sources. *Mineralium Deposita*, **53**,323-338.
- TATSUOKA, M. M., & LOHNES, P. R. (1988). *Multivariate analysis: techniques for educational and psychological research* (2nd ed.). Macmillan publishing co, inc.
- TOWNLEY, B. K., HERAIL, G., MAKSAEV, V., PALACIOS, C., DE PARSEVAL, P., SEPULDEVA, F., ORELLANA, R., RIVAS, P. & ULLOA, C. 2003. Gold grain morphology and composition as an exploration tool: application to gold exploration in covered areas. *Geochemistry: Exploration, Environment, Analysis*, **3**, 29–38.
- TREMBLAY, L.P. 1982. Geology Of The Uranium Deposits Related To The Sub-Athabasca Unconformity, Saskatchewan *Geological Survey Of Canada, Paper 81-20*. 51p.
- WILKINSON, J.,J., BAKER, M.,J., COOKE, D.,R., & WILKINSON, C.,C., 2020. Exploration Targeting in Porphyry Cu Systems Using Propylitic Mineral Chemistry: A Case Study of the El Teniente Deposit, Chile; *Economic Geology*, **115** . 771-791.
- WATLING, R.J., HERBERT H.K., DELEV, D. & ABELL, I.D. 1994. Gold fingerprinting by laser-ablation inductively coupled plasma- mass spectrometry. *Spectrochimica Acta* **49**, 205-219.

- WILDE, A.R., BLOOM, M.S, & WALL, V.J. 1989, transport and deposition of gold, uranium and platinum group elements in unconformity-related uranium deposits: *Economic Geology Monograph*, **6**, 637-660.
- YOUNGSON, J.H. & CRAW, D. 1995. Evolution of placer gold deposits during regional uplift, central Otago, New Zealand. *Economic Geology* **90**, 731-745.
- ZAYKOV, V.V., MELEKESTSEVA, I.Y., ZAYKOVA, E.V., KOTLYAROV, V.A. & KRAYNEV Y.D. 2017. Gold and platinum group minerals in placers of the South Urals: Composition, microinclusions of ore minerals and primary sources. *Ore Geology Reviews* **85**, 299-320.
- ZUO, R. 2011 Identifying geochemical anomalies associated with Cu and Pb–Zn skarn mineralization using principal component analysis and spectrum–area fractal modeling in the Gangdese Belt, Tibet (China). *Journal of Geochemical Exploration*. **111**, 13-22.
- ZUO, R., CARRANZA, E.J. & WANG, J. 2016 Spatial analysis and visualization of exploration geochemical data. *Earth-Science Reviews*. **158**, 9-18.

ACCEPTED MANUSCRIPT

Figure Captions

Figure 1. Features of polished gold particle sections. Detrital particles unless otherwise stated. A-F BSE images. A: variation in Au-Ag ratio indicated by greyscale with order of alloy formation indicated. Sperrin Mountains, N. Ireland. B: Inclusion in gold liberated from hypogene setting, Lone Star, Klondike, Yukon, Canada. C: Paragenesis of gold particle indicated by high Ag core partially replaced with high-Ag alloy containing inclusions of wittichenite (CuBiS_3), Ochil Hills Scotland. D: Heterogeneity of Au-Ag alloy resulting from grain boundary migration, post precipitation, Sperrin Mountains, N. Ireland. E: Pure Au infilling cracks sympathetic to grain boundaries, Clear Creek, Yukon, Canada. F: Homogenous grain core surrounded by Au rim, with apparent thickness controlled by particle orientation, Cariboo Gold District, BC, Canada. H-K of gold particle from Similkameen River, BC, Canada. G: SE image (i) and BSE image (ii) of the same impacted zircon particle in a polished section of a gold particle. Note contrasting textures of gold/'inclusion' contact in Figures 1B and 1G. H: BSE image of surface post analysis by ToF-LA-ICP-MS, showing pyrite inclusions and two other unidentified inclusion types (A and B) not recorded during routine visual screening. 'A' contains Fe and trace Bi, and 'B' contains Te and trace Fe. I-K: Images of a ToF-LA-ICP-MS maps for Pd, Fe and Ir (reproduced with permission from Banks et al. 2018). Element abundance is represented by 'intensity' rather than a quantitative value (see discussion in Chapman et al. 2021). I: alloy is heterogeneous with respect to Pd, but Pd is present on much of the section. J: localised high intensity of Fe indicates presence of mineral inclusions (compare with Fig 1H). K: Single, localised high concentration of Ir (bottom centre) provides an example of a 'cluster'.

Figure 2. Graphical methods used to depict alloy concentrations in gold particles. A: triangular diagrams using scaling of minor alloying elements to generate compositional fields. (Adapted from Townley 2003, with additional data from Bonev et al. (2002)). B: cumulative percentile plots showing typical responses from a hypogene source (BRX zone) and gold from adjacent placer. (Data from Chapman et al. 2018). C: Bivariate plots permitting multi-variate analysis through use of symbols to depict other variables. (Data from Chapman et al. 2018)

Figure 3. Characteristics of detrital gold particles from magmatic hydrothermal systems. All micrographs are BSE images. A,B: Description of Ag contents and inclusion assemblages of gold from calc alkalic and alkalic porphyries in BC and Yukon, Canada (data from Chapman et al. 2017; 2018). Dashed lines indicate sample is derived from crushed ore. C-D: typical inclusion species C: Revenue Creek, Yukon, Canada, D: Friday Creek, Copper Mountain area, BC, Canada, E: Rude Creek, Yukon, Canada. F-I Description of Ag contents and inclusion assemblages of gold from low and intermediate sulphidation epithermal systems F: examples of wide compositional range in Ag between populations from different localities (data from Chapman and Mortensen 2006; Chapman et al. 2018). H and I: typical inclusion species H: gold liberated from hypogene sample, Black Dome, southern BC, Canada, I: Gold particle from Ochil Hills, Scotland showing an unaltered Bi-telluride inclusion and another which has been oxidized to Bi carbonate through fluid ingress. J: Example of molybdenite inclusion in gold from an intrusion-related system, Dublin Gulch, Yukon, Canada. K and L

textures and inclusions typical of gold associated with ultramafic lithologies, placer particles from Wheaton Creek, BC, K: exsolution texture of tetra auricupride from Au-Ag-Cu alloy. Particle also exhibits a Au-rich rim. L: chalcocite inclusions in Au-Ag-Cu alloy. M: Au-PGM association in PGM particle from lower Orange River, Namibia.

Figure 4. Characteristics of detrital gold particles from orogenic hydrothermal systems. A and B: (data from Chapman et al. 2010a, Naden and Styles 1994). Dashed lines indicate sample is derived from crushed ore. A: range of Ag profiles in terms of shape and Ag value depicting gold from both hypogene and placer settings. Lone Star and Nugget Zone samples derived from in situ mineralization, Lone Star area, Klondike, Yukon. Gay Gulch and Adams Creek are placer localities in the environs of the Lone Star deposit. Eureka Ck (Yukon) and Kwekwe (Zimbabwe) are placer localities. Data from Naden et al. 1994, Chapman et al. 2010a, Chapman et al. 2011. C-F: BSE images of typical inclusions. C and D: Leadhills, Scotland, E: Blueberry Creek, Yukon, Canada, F: Nkol Medoum, Cameroon.

Figure 5. Characteristics of detrital gold particles from redox controlled low temperature oxidizing chloride hydrothermal systems. A and B: Ag and Pd profiles of gold particles from three different regions, data from Chapman et al. (2009). C and D: examples of intermetallic compounds that are commonly observed within Au alloy. C: River Ayr, Scotland and D: River Dart, Devon, E Example of Se-bearing inclusions in Au alloy, Glengap Burn, Scotland. E: examples of characteristic gold morphology ranging from pristine dendrites to waterworn particles which retain evidence of their original morphological features. Images i-iii: Devon, England. Images iv, v: Lammermuir Hills, Scotland.

Figure 6: Results of synthetic minority oversampling technique to overcome class imbalance. Blue data points are synthetic, and red data points are natural. Note that all synthetic datapoints plot within the range dictated by the natural data points.

Figure 7: An example of one classification tree from within the Pythagorean forest. The white squares represent branches sharing multiple deposit types, A: green segments represent data from orogenic deposit types. B: blue segments represent alkalic porphyry deposit types. C: red segments represent low sulphidation epithermal deposit types. D: synthesis of figures A-C.

Table Captions

Table 1. Summary of mineralogical characteristics of gold particles formed in different styles of mineralization

Table 2: Machine Learning Model evaluation results. The Random Forest model returned the highest 'area under curve' (AUC), classification accuracy (CA) and test accuracy (F₁ score).

Style of mineralization	Mineralization/Microchemical signature				Comments
	Alloy compositions		Inclusion suite		
	Ag range wt (%)	Other metals	Chemistry	Typical Mineralogy	
Orogenic: Phanerozoic ¹⁻⁷	4-30	Occasional Hg to 10%	i.S, ii. S+As iii.S+Te±As±Ag iv. Pb+S+Sb±As	i. py, ga, cpy, sph ii. py, ga, cpy, sph, apy iii. py, ga, cpy, sph, hs, apy iv. ja, ga, apy, py	Simple sulphide inclusion suites are the most common. Te usually present as hs.
Orogenic: Precambrian ^{8,9,10,11}	5-50, but many <10	Cu to 2% common Occasional Hg to 3%	S,±As, ± (Te+ Bi)	py, ga, cpy, sph, apy ±BiTe	The majority of alloy compositions are in the 1-10 wt% Ag range
Epithermal: Low sulphidation ^{12,13,14}	1-50	Occasional Hg to 10%	S, ±As,+Te,+Ag, Bi,	py, ga, cpy, sph, BiTe ±apy	Large variation in Ag ranges in populations from different localities but often small variation between particles from a single locality. Cu normally below LOD by EPMA (0.02 wt. %)
Epithermal High Sulphidation ^{15,16}	1-14	Cu to 1wt%	Cu+Pb+Zn+S+As±Te	bn, cc, cpy, ga, sph	Limited data available
Calc alkalic Porphyry, ¹⁴	5- 50	Cu usually > 0.02 wt.% (LOD by EPMA)	Bi+Pb+Te+S		
Alkalic porphyry ¹⁷	5-40	Hg, Pd to 11wt% in around 4% of particles	Hg+Pd+Pb+ Bi+Te+ Cu	tem, PdTe, PdAs, py, cpy, bn, cc,	
Skarn ¹⁸	>11		Pb+Ag+Te+Bi+S		Limited data available
Oxidising chloride hydrothermal : low temperature (T< 120°C) ¹⁹	0-6	Pd or Hg to 12%, Rare Cu to 4%	Se±Te+ wide range of metals	Selenides and tellurides of Pd, Hg, Cu, Bi, Pb. pt	Ag often extremely low. Au-Pd alloys common. Sulphides absent from high Au and Au-Pd alloys
Ultrabasic intrusion association ²⁰	0-20	Cu commonly to 10 wt.%)	Au,Cu	Au-Cu intermetallics, cc, po	Common exsolution texture of Au-Cu intermetallics from Au-Ag-Cu alloy. Often extreme heterogeneity so ascribing a Ag value is problematic

1: Chapman, et al. (2000a), 2: Chapman et al (2000b), 3: Chapman et al. (2006), 4: Chapman et al. (2010a), 5: Chapman et al. (2010b), 6: Moles et al. (2013), 7: Chapman and Mortensen 2016, 8: Henney et al. (1994) 9: Omang et al (2015), 10: Dongmo et al. 2018, 11: Chapman et al. (2021) 12: Chapman et al. 2005, 13: Chapman and Mortensen 2006: 14: Chapman et al. (2018), 15: Bonev et al. (2002), 16: Naden and Henney, 1995, 17: Chapman et al. (2017), 18: Potter and Styles, (2003), 19: Chapman et al (2009), 20: Knight and Leitch (2001)

Key to symbols: apy=arsenopyrite, Au-Cu = copper gold intermetallic compounds BiTe= undifferentiated Bi tellurides, bn=bornite, cc= chalcocite, cpy=chalcopyrite, ga= galena, hs= hesite, py=pyrite ja= jamesonite, pt= potarite PdAs= undifferentiated palladium arsenides, PdTe= undifferentiated palladium tellurides, sph= sphalerite, tem= temagamite

Table 1

Model	AUC	CA	F ₁	Precision	Recall
kNN	0.841	0.734	0.725	0.737	0.734
SVN	0.793	0.672	0.615	0.744	0.672
Random Forest	0.930	0.840	0.839	0.839	0.840
Neural Network	0.871	0.764	0.783	0.783	0.764
Naïve Bayes	0.869	0.739	0.743	0.743	0.739

Table 2

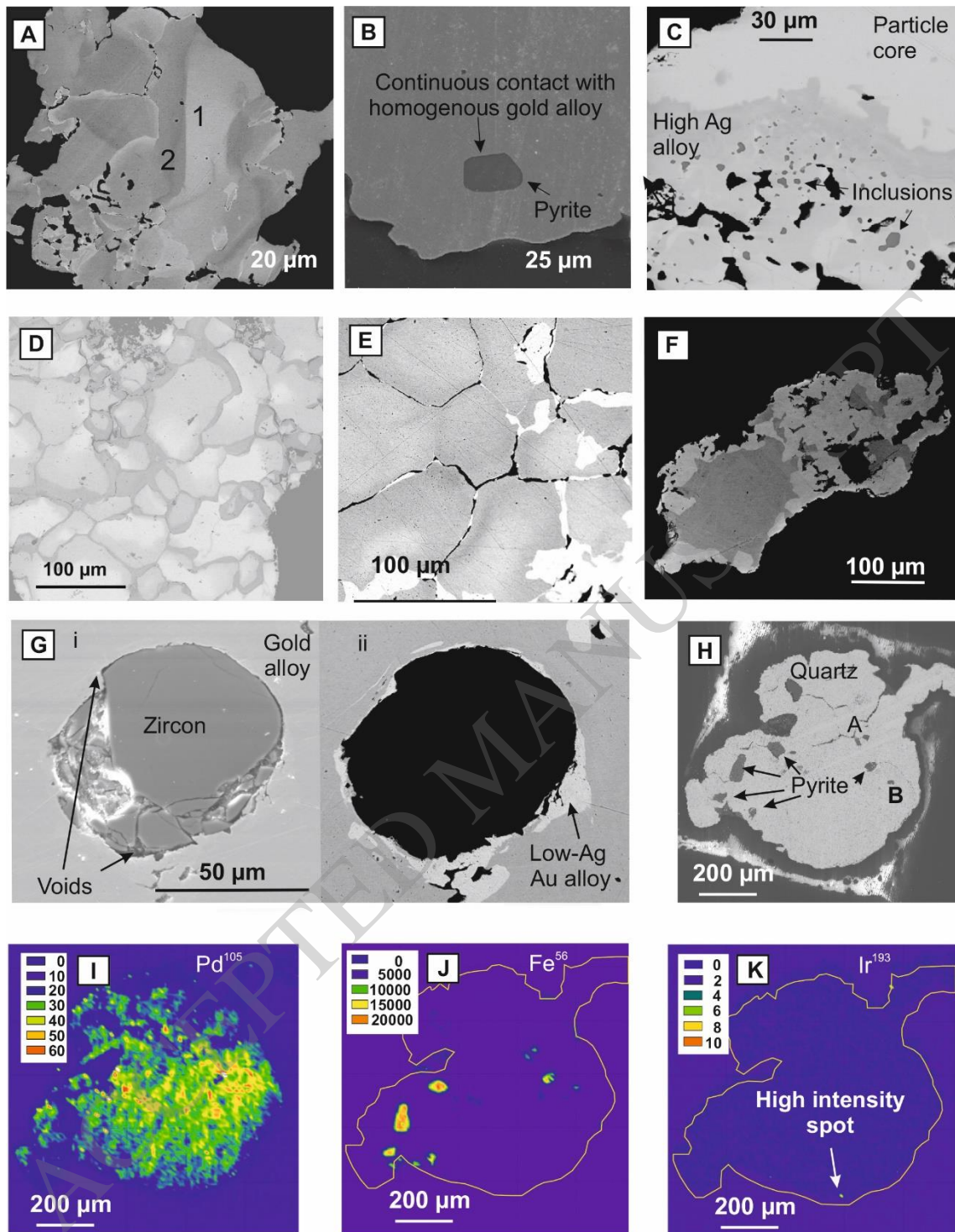


Figure 1

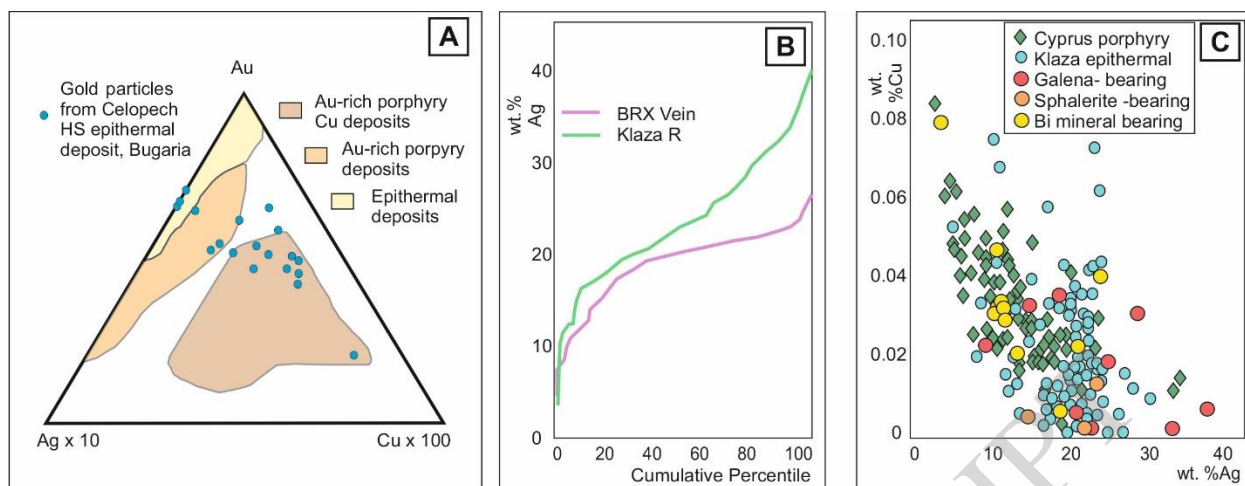


Figure 2

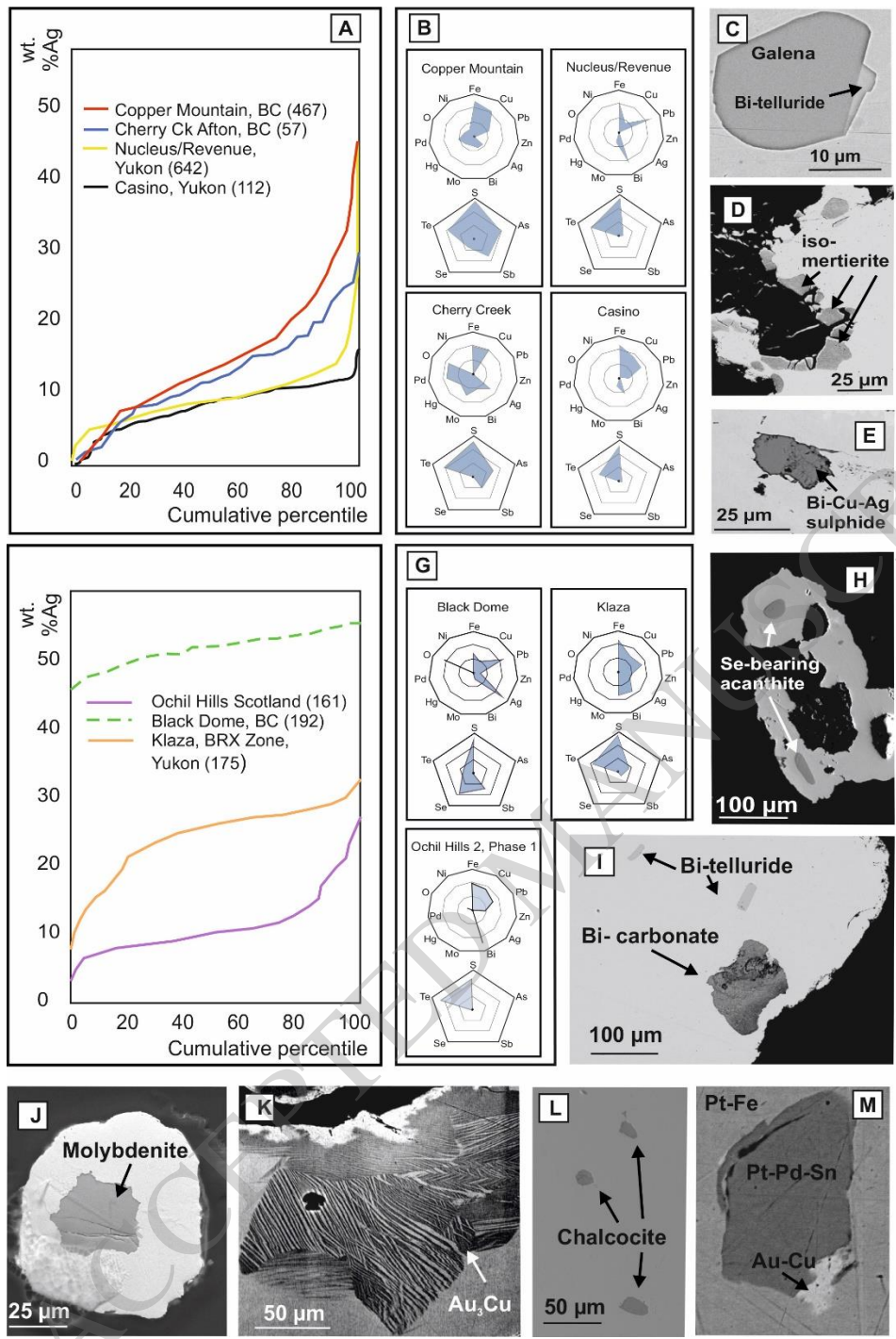


Figure 3

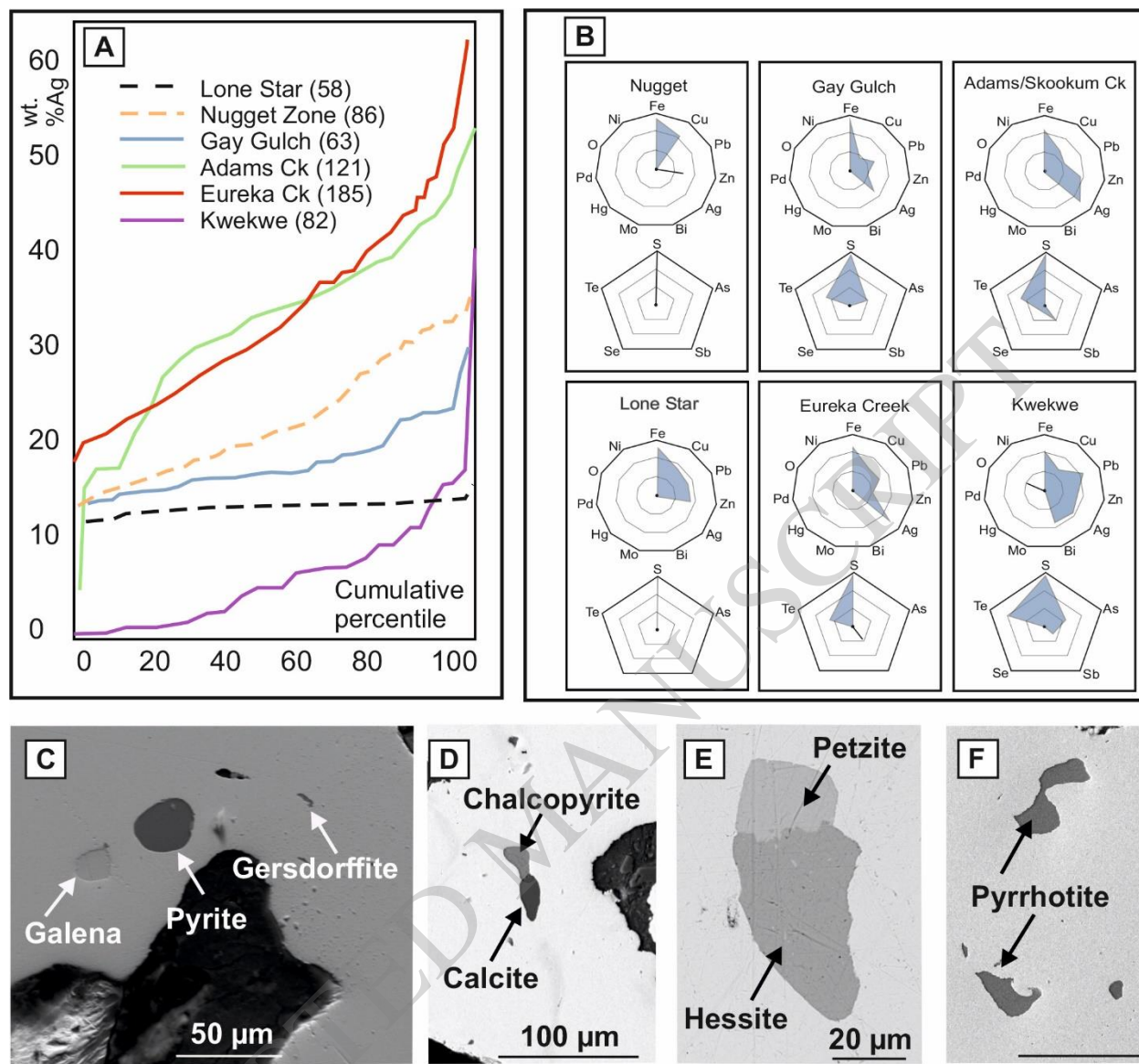


Figure 4

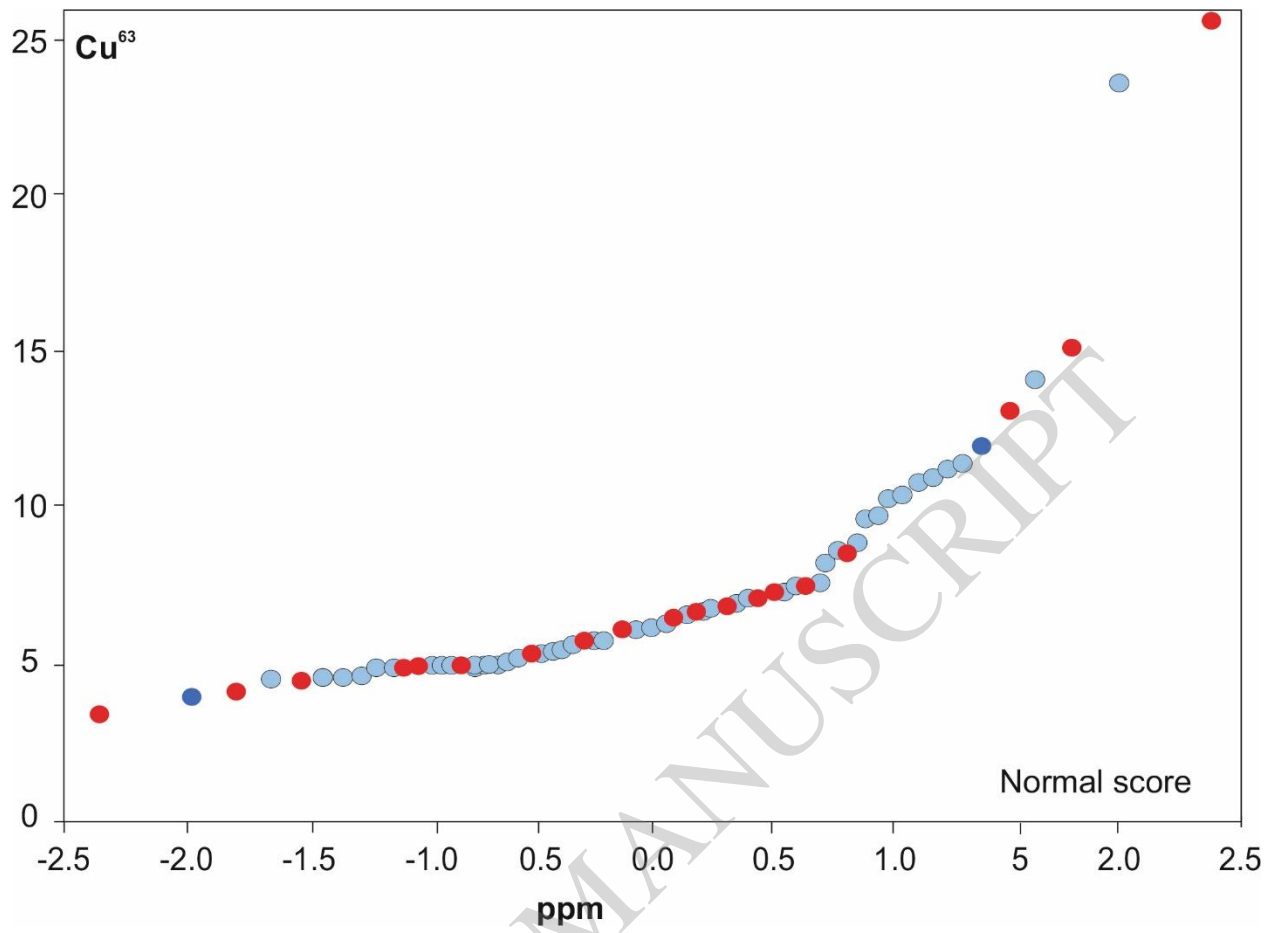


Figure 6

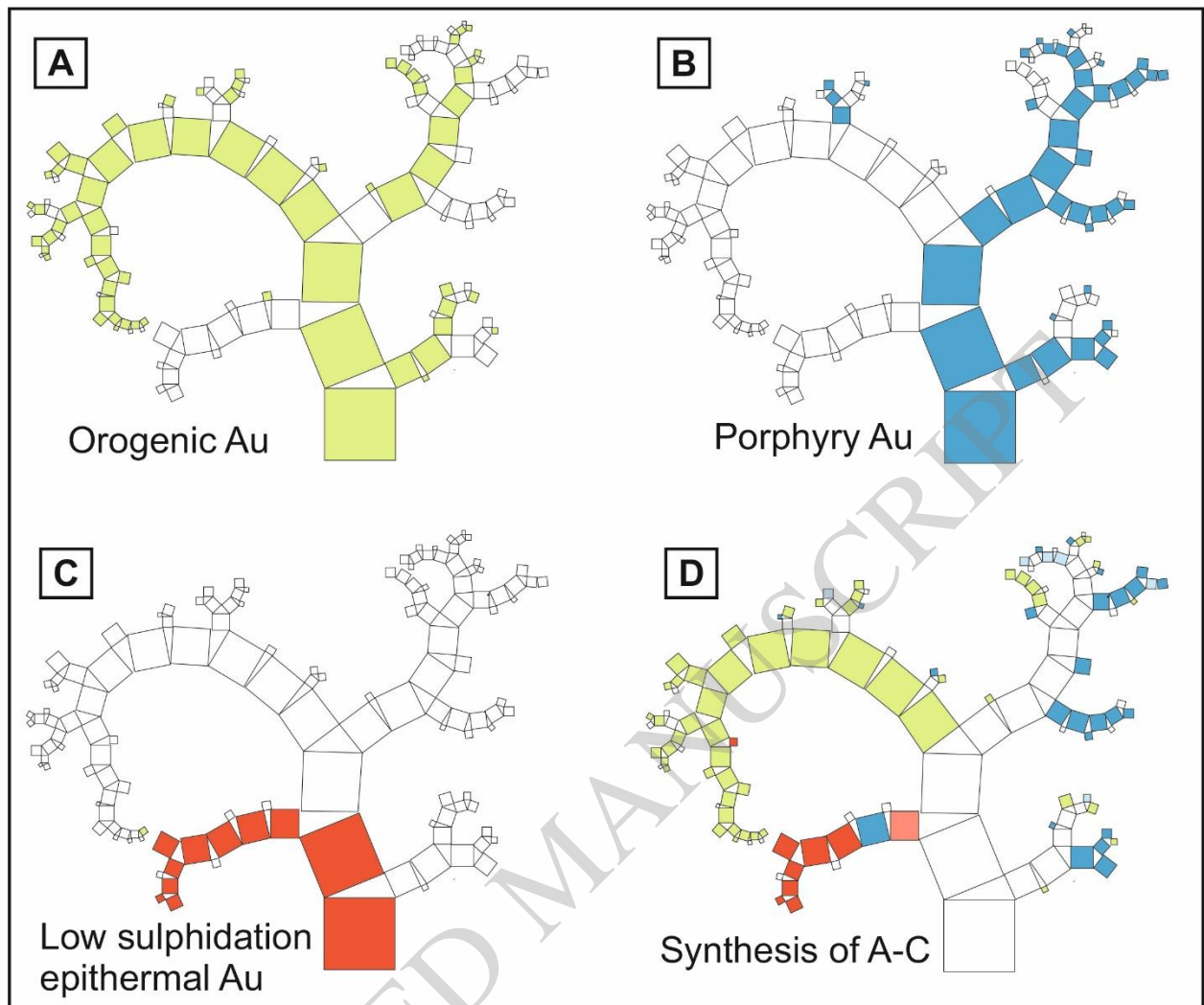


Figure 7